

Reply to the comments from anonymous reviewer and Daniel Schillereff. on the manuscript (HESSD-2019-415) " New flood frequency estimates for the largest river in Norway based on the combination of short and long time series" by Kolbjørn Engeland, Anna Aano, Ida Steffensen, Eivind Støren, Øyvind Paasche

We are very grateful for the excellent reviews afforded by the from anonymous reviewer Daniel Schillereff which we believe will improve our paper. Below you find a point to point replay to all comments and the changes in the manuscript are indicated.

Please note that we refer to page and line numbers in the manuscript with tracked changes.

Reply to the comments from the anonymous reviewer

Comment from the referee

Length of the paleoflood record: It is not clear how the authors state the value of 10 300 years from the sediment core. Is it the first dating of a sediment? If yes, according to the dating uncertainty (see a discussion in Dezileau et al., 2014, *Geomorphology*, 10.1016/j.geomorph.2014.03.017), it may be better to round it to 10 000 years. Another option is to refer to the huge glacial lake outburst flood (reported in section 5.1). It may be the beginning of the paleoflood record. Hogaas and Longva (2016) postulated a date of 10 000 – 10 400 years. So again, a rounded value of 10 000 years may be preferable.

Author's response

The value of 10 300 comes from Table 5 where the calibrated age based on 14C-dating of the lowest sample is 10259 – 10403 BP (68 % C.I.). We therefore think that 10 300 is a reasonable and robust assessment of the age of the lowest part of the sediment core based on the data used in this study. The paper by Høgås & Longva (2016) does not contradict our age assessment but suggest that the lowest part is not older than 10 400 years. Note that the age estimate provided by Høgås & Longva (2016) comes with considerable uncertainty as well.

Author's changes in manuscript

We keep our age assessment of 10 300 years. To support this age assessment, we have added reference to Table 5 and Figure 11 in the first paragraph of section 4.1 (Page 14, Line 24-25)

Comment from the referee

Section 1: Page 2, line 3: the main reason for the increasing of flood damages is the increase of economic values within the flood plain. Impact of climate change is of concern, but do not forget that flood risk has two components: flood hazard and flood exposure.

Author's response

We agree that a main reason for the increasing of flood damages is the corresponding increase of economic values within the flood plains.

Author's changes in manuscript

We have added this important clarification in the first sentences of section 1. (Page 2, line 3-4)

Comment from the referee

Figure 2 left: put one curve with dash lines (easier to follow)

Author's response

In the figure on the left hand side of Figure 2, we follow the suggestion by the reviewer and add dashed lines. We will also use different colors in order to increase the contrast between the two.

Author's changes in manuscript

We have changed Figure 2 (Page 5)

Comment from the referee

Page 5, line 5: is the beginning of the Holocene period in Norway exactly 11 700 years ? Give a reference.

Author's response

The beginning of the Holocene period is in most literature referred by 11 700 years B.P. See e.g Walker et al (2009).

Author's changes in manuscript

We have added the reference to Walker et al (2009) in the first sentence of section 2.2. (Page 5, Line 17)

Comment from the referee**Section 3**

Page 3, lines 8-11: it is not clear within section 3.1 which systematic period is considered. It is written 1871-1937, but in fact, floods larger than $x_0 = 2533 \text{ m}^3/\text{s}$ have been used (table 1: years 1966, 1967, 1995). If the flood regime was affected by river regulation after 1937, we expect to introduce a correction on the three largest floods after 1937. If not, you can consider the whole period 1871-2019. Please provide the p-value of a statistical test (e.g. Mann Kendall test) with the two periods: 1871-1937 and 1938-2018.

Author's response

The period with systematic streamflow data started in 1872. We used data for the period 1872 - 1936 to avoid effects of river regulations on the flood peaks. We did not use the floods from 1966, 1967 and 1995 in the flood frequency analysis. These floods are, however, listed in Table 1 since they are documented on the flood stone. It could be an option, but would require a detailed hydraulic model, to recreate the catchment dynamics with no river regulations. This is beyond the

scope for our study. The mean annual flood for the period 1872 – 1936 is 1700 m³/s. For the period 1937-2019 it is 1362 m³/s. A Wilcoxon test indicates that this difference in mean value is significant with a p-value of $2 \cdot 10^{-8}$ for the zero-hypothesis (i.e. no difference in mean values between the two periods).

Author's changes in manuscript

In section 3.1 we have specified that we used only systematic flood observations for the years 1872-1936 (Page 8, Line 3) and added the results of the Wilcoxon test (Page 8, Line 5-6).

Comment from the referee

Page 10, lines 10-21: Stability of the geometry of the Glomma river is discussed in section 5.1. May be here in section 3.2.1 or in section 5.1, you could add information on the gaugings. Is the rating curve stable or do we need to use a set of different rating curves according to the gaugings?

Author's response

The stability of the river profile at Elverum is an important assumption when we assess the discharges of the historical floods. The gauging station was moved around 660 meters in 1969. For the period 1872 – 1968 only one rating curve is used. For the period 1969-2020, the rating curve changed following the flood in 1995. In our study, it was assumed that the river profile at Elverum was stable for the historical period and that the flood in 1789 did not make any substantial changes. This seems to be a reasonable assumption since four large floods occurred during the period 1872 - 1968. We will add a small discussion on this topic to the revised paper. The stability of the river profile at Kongsvinger where the bifurcation event takes place is also an important assumption that is discussed.

Author's changes in manuscript

We chose to add this information in the discussion in section 5.1. (Page 23, Line 6-10)

Comment from the referee

Section 4.3: It is not easy to follow the different options of computation for flood frequency analysis:

- Systematic period: is it 1871-1937 (section 3.1) or 1872-1936 (section 5.3)?
- Historical period: 1653-1872. It may end in 1870 or 1871
- Paleoflood period: 1320-1850. Explain the starting date 1320. If paleoflood and historical floods are in agreement during the overlapping period, we expect to have 1320-1652

Author's response

The different periods of data used in the flood frequency analysis are as follows

- Systematic data used for flood frequency analysis is 1872 – 1936
- Historical flood data is 1653 – 1871, a length of 219 years
- Paleo-period lasted from 1300 – 1652, i.e. a length of 352 years with 110 flood events in total when we combined paleo- historical and systematic data.

- The paleo record lasted from 1300 – 1871, a period of 571 years with 208 floods when we combined paleo and systematic data.

The oldest historical flood was observed in 1675. The average waiting time between the historical floods are 22 years. The start of the historical period was therefore set to $1675 - 22 = 1653$ as recommended by Prosdocimi (2018) and Engeland et al. (2018).

We decided to let the paleo-periods start in year 1300, since we have a quasi-stationary period from 1300 until today. Before 1300 the flood frequency is small. We will slightly change the length of the paleo-periods so that they both start in year 1300 and ends the year before the systematic record starts or the start of the historical period.

Author's changes in manuscript

We have modified section 4.3 and added Table 6 that summarize the different data sources and periods used for the flood frequency analysis. (Page 22 and 23)

Comment from the referee

Plotting positions for figures 14 and 15 are not explained. According to Hirsch and Stedinger (1987), you should consider ALL the floods larger than the threshold x_0 over the historical + systematic period, and then the systematic floods lower than x_0 . We expect to find a set of 14 peak flows (11 from historical period + 3 from the systematic period), and the remaining annual maximum values lower than x_0 for the systematic period.

Plotting position of the 1789 flood should be different, according to option 1 or 2 (largest flood since 1653 or since 10 000 years).

Author's response

The plotting positions in Figure 14 and 15 are based on Hirsch and Stedinger (1987) that is based on the Cunnane plotting position (Cunnane 1978) the exceedance probability p_i of x_i with rank i from a data set with t historical floods representing the historic period h , and s systematic floods with e extraordinary floods is given as:

$$p_i = \frac{i - 0.4}{l + 0.2} \cdot \frac{l}{n} \quad i = 1, \dots, l$$

$$p_i = \frac{l}{n} + \frac{n - l}{n} \cdot \frac{i - l - 0.4}{s - e + 0.2} \quad i = l + 1, \dots, t + s$$

where i is the rank, l is the number of extraordinary floods ($l = t + e$) and n is the length of the period for which we have information about floods (note that $n = h + s$)

Since we used the systematic streamflow data from 1872-1936, we have 2 systematic floods exceeding the threshold (1916 and 1934) (i.e. $e = 2$) and 9 historical floods (i.e. $t = 9$ and $l = 11$) for the period 1653 - 1871. The length of the systematic record $s = 65$. The length of the historical period $h = 219$ years, thus $n = 284$ years. We did not include the floods from 1966, 1967 and 1995.

The plotting position for the highest flood is 292 years and agrees well with the Figs. 14 and 15.

Author's changes in manuscript

We have added section 3.4.2 that summarize the plotting position. We refer to 3.4.2 in the captions of Figure 14 and 15.

(Page 13 line 36-41 and Page 14 line 2-3)

Comment from the referee

On figure 5, it is not easy to understand which curves relate to cases (i), (ii) and (iii) vs systematic floods included, all floods included, paleoflood included.

Author's response

We think this comment refers to Figure 15. We agree that this is unclear and have improved the Figure captions and the text and also added Table 6 that summarize the period for all data sources.

Author's changes in manuscript

The caption of Figure 15 is improved as well as the text summarizing the results. (Page 22, line 7-22). We have also added Table 6 that summarize the time period covered for all data sources.

Comment from the referee

Section 5.2

On figure 17, it is very interesting to see the flood rich period during the LIA with low temperature (and the contrary before 500 cal. yr BP). The authors could add a comment on the fact that we have two peaks during LIA but the temperature did not significantly change.

Author's response

The two sub-periods with increased flood peaks during the LIA are indeed interesting, and we thank the reviewer for pointing this out. During this period the average summer temperature for the northern hemisphere did not change substantially. To interpret the dip in flood frequency around year 400 BP remains challenging. Firstly, the temperature anomaly represents an average for the northern hemisphere and not for south-eastern Norway in particular. Secondly, the combination of winter temperature and precipitation might be even more useful for interpreting the flood frequency. Such proxy information is not yet available and therefore limits the possibilities to fully what we observe.

In the revised paper we will add more discussion on flood generating processes and how the available proxy-data can assist us in interpretation of the non-stationarity observed in the paleo-record. See also our answers to Reviewer #2.

Author's changes in manuscript

We have modified the discussion in section 5.2 (Page 25, lines 24-26)

Comment from the referee

Section 5.3

Page 26, line 6: it remains unclear how the 600 year period is chosen. Additionally, according to section 4.3, it is rather a 530 year period (1320-1850) or a 332 year period (1320-1652)

Author's response

We agree that this part of the text explaining how the period for the paleo-data was chosen is a little confusing and we will make an effort to improve the clarity as explained in an earlier comment.

Author's changes in manuscript

We have changed the 6th paragraph in section 5.3 (Page 29, line 27)

Comment from the referee

Small typos

Page 2, line 18: they require that buildings

Page 2, line 22: up to 1000-year floods... (see Lovdata, 2010, and TEK17, 2018 for regulations)

Page 3, lines 24-25: (Hanssen-Bauer et al., 2017)

Page 5, line 16: the flow direction reverses

Page 5, line 24: in Fig. 5

Page 6, line 6: (after Hegge, 1968)

Page 10, line 4: reference of Ostmo (1985) is missing in section 7

Figure 8: Legend "Max discharge"

Page 11, line 2: (Renberg and Hansson, 2008). Samples

Page 11, line 39 add "if $k=0$ (Gumbel distribution)" on the second part of equation (1)

Page 22, line 18: A second assumption is that the river

Page 22, line 20: Hogaas and Langva (2016) give an age of 10 – 10.4 cal ka BP in conclusion

Page 22, line 22: Based on Klæboe (1946) and Hegge (1968) the threshold

Page 22, line 26: According to Hegge (1968), the... in 1967 CE

Page 22, line 38: and regional

Page 23, line 15: reference of Moberg et al. (2015) is missing in section 7

Page 24, line 14: Velle et al., 2010

Page 24, line 22: and in the central alps

Page 25, line 4: Storen et al. (2012)

Page 26, line 10: the threshold for historical floods is too low

Page 27, line 25: 7. References

Author's response

We have corrected all these typos in the revised manuscript.

Author's changes in manuscript

We have corrected all these typos in the revised manuscript

Reply to the comments from Daniel Schillereff

Comment from the referee

Comment #1: Structure and content of the introduction : Given the broad audience of HESS, and the likelihood that some (many?) readers may be more accustomed to studying recent datasets, I suggest the authors incorporate more detail on the palaeodata in the introduction. I specifically suggest the authors elaborate on the ways in which palaeo data can help address the “two reasons” outlined on Page 2, Lines 23-26. Whilst many readers will have a sound knowledge of return periods and design flood estimates, applying palaeo data to these processes – and the value of doing so - may be quite new.

Similarly, I think it would be useful for the authors to say more about the timescales involved: how far back in time can palaeohydrological data be obtained from lake sediments (page 2, lines 42-43) and historical records (page 3, lines 5-11)? This would give readers a platform of knowledge that will be helpful when they engage with the return period calculations later in the paper. Likewise, I think the objectives (Page 3, lines 39-43 and on to Page 4) could be a bit more specific and pay particular attention to the timescale of your analysis

I also query whether Page 3, lines 5-11 could be slimmed down. To keep the focus on your work, perhaps mention briefly that there are a range of historical archives but place particular emphasis on epigraphic sources – especially flood stones - as that is the sort of data used later in this study

Author's response

The suggestions for modifying the introduction are very useful and we will include changes in the revised manuscript.

We will, as suggested, provide more details on how paleo-data can help to reduce uncertainty associated with flood prediction (more data leads to smaller estimation uncertainty) and provide additional insight to flood variability on longer time scales, which can further advance our understanding of how climate change influence flood variability on multiple time scales.

We will also add more information about the time scales involved. Although we do not aim to give a review of different archives suitable for paleoflood reconstructions (e.g. Wilhelm et al., 2018), we will nevertheless include info on the length of historical records (back to the 16th century) and lake sediment archives (Holocene) available in Norway.

Author's changes in manuscript

We have modified the introduction (Page 3, Line 5 – 18)

Comment from the referee

I am pleased the authors mention the possibility that changes in land-use could play a role and, similarly, I was really pleased that the authors explicitly assess whether the fluvial system behaviour would have allowed bifurcation events throughout the Holocene (Page 22, Lines 18-30). I think there is scope to go further in ruling out the possibility that changes in flood frequency are driven by rather than amplified by human activity.

Page 3, line 24: it is important to state here that non-stationarity needn't only be a response to climatic variability. Human alteration of the land surface can also create a non-stationary fluvial system.

Page 5, Lines 2-5 talk about ‘noteworthy land-use changes during the last 400 years, and specifically the removal of woodland cover’. This is returned to briefly on Page 25, Lines 6-15

but I think this needs a more critical and in-depth evaluation. The authors acknowledge, for example, the notable rise in flood frequency rises around 500 yr BP, which happens to coincide with the assertion on Page 25 Line 8 “The mining industry that started in Norway in the 16th century required a large amount of timber which resulted in widespread deforestation also in Glomma’s catchment”. How confident are the authors that widespread deforestation amplified the climate driver but was not a driver of sedimentological change in its own right?

Similarly, I think the interpretation of external drivers, especially through the 2500-4000 yr BP flood-rich period, would be strengthened considerably if human interference could be ruled out. In Britain, for example, a number of fluvial and palaeolimnological studies show widespread mobilisation of sediments at that time resulting from settlement expansion. I have no idea about the mid- to late-Holocene history of human occupation in southern Norway but presenting or referring to data ruling this out possibility would really strengthen the case.

Author's response

Human modifications of the landscape are also important factors for future flood risk and we will add this information to the introduction.

The issue of human influence on the landscape is in this case two-fold and may or may not have sedimentological as well as hydrological influences on the system in question. Changes in land-use and deforestation can impact sediment availability in the catchment, but it can also change the buffering capacity and hence the run-off regime. We believe that the land-use changes caused by the removal of woodland cover that started in the 16th century may have influenced the local erosion and sediment transport of the upstream Glomma catchment (though, note that no data presently exists here), but because this area represents only a fraction of the total catchment area we think that these ‘excess sediments’ would be diluted downstream. Another relevant point here is that the downstream gradient of the river Glomma is not steep so sediments can easily be deposited long before they reach the bifurcation point at Kongsvinger. A final point here is that the sediment source for the flood layers deposited in Flyginnsjøen is suggested to be mainly local, and the area around the lake and the location for the bifurcation events itself was not subject to removal of woodland for mining which would reduce the potential influence of anthropogenic influence on the sedimentary budget.

Having said that, we do not rule out the possibility that the removing of woodland since the 16th century amplified the size (and frequency) of floods since forests, in most cases, reduces flood peaks. This, however, require a more regional and systematic vegetation change than that related to mining in the upper Glomma catchment to affect the 154450 km² large catchment. The 2500-4000 yr BP flood-rich period coincidence largely to the bronze age (2500-3700 BP) when settlements and farming expanded in Norway. We see, however, similar flood rich period in other lake sediment records that certainly not are influenced by farming (shown in Fig. 18) and argue that the effect of land-use cannot explain the observed changes in flood frequency. Se also reply to comment #4 on this matter.

Author's changes in manuscript

We have modified section 5.2 in the discussion chapter (Page 27, Line 20 – Page 28, Line 8).

Comment from the referee

Comment #3: Evaluating the geochemical flood proxy

Overall, I find the proxy reconstruction to be convincing. I do wonder whether it could be strengthened by providing some information on the geochemical composition of the glacio-fluvial material between the two lakes. The authors state the Glomma catchment is the largest in Norway. To what extent will sediments being deposited in Flyginnsjøen during a bifurcation event be mixed with material entrained elsewhere in the Glomma catchment?

I commend the authors' application of a rigorous peak detection algorithm and critical assessment of the fidelity with which the sediment record matches the gauged (post-1953) flood record. However, I found Figure 12 and the associated text a bit difficult to follow. For example, Page 18, Lines 12-15 the authors highlight that, overall, there is a good match but also segments that do not correspond, but this analysis would be strengthened had it was easier to figure out which XRF peak linked to which flood volume bar. One idea would be to colour the vertical flood volume lines and the circle/cross shapes one of two colours when you are confident in their stratigraphic correspondence and the other colour when a match is more difficult to establish. A minor point but, personally, I think the dashed vertical lines denoting each year add substantial clutter to the graph and could be removed. Overall, Figure 12 makes a really important contribution to the paper but it's complicated and uses many different colours and shapes. Improving its aesthetics would really strengthen the paper.

Author's response

We agree that a more thorough sedimentary analysis of potential sediment sources in the catchment could add valuable information to the composition of the recorded flood deposits, and perhaps even denote source areas and thus also flood triggering mechanisms (see eg. Støren et al 2016). Given the size of the Glomma catchment, and the mixing process involved such an approach will require not only sediment samples from the area between the bifurcation threshold and the lake, but also representative samples from potential sedimentary sources in the 154450 km² catchment for comparison. This would be an interesting exercise, but the workload would be enormous and is well beyond the scope of this paper.

Moreover, during bifurcation events the discharge in the Flyginnsjøen catchment increase with an order of magnitude, dramatically changing the erosion in the area. This change is deemed to mask subtle variability in sediment transport for the Glomma catchment.

Linking the sedimentary signal to specific individual flood events is, as the reviewer recognizes, challenging, and it's equally challenging to visualize this link in figure 12. We agree that the dashed vertical lines are not serving any good purpose and have removed these. The suggestion made by the reviewer to add color coding on peaks where we "are confident in their stratigraphic correspondence" is more problematic. Firstly, the plot is already busy, and more colors will add more clutter and probably not improve readability. Secondly, considering the uncertainties in the age-depth model we have not (yet) found a good way to estimate probabilities for correspondence either. Consequently, we rest on the assumption that our 23 recognized peaks in the sedimentary signal corresponds to the 24 bifurcation events over the same period. We argue that this, and the visual correspondence between peaks in K and Ti and peaks in discharge shown in fig 12 are sufficient show causality between bifurcation events and the observed sedimentary signal.

Author's changes in manuscript

The discussion on uncertainties in the age-depth model and the correspondence between the historical flood events and the sedimentary signal have been elaborated on in section 5.1 in the discussion (Page 23, line 18-22) and we have improved the aesthetics of figure 12 (Page 19).

Comment from the referee

Comment #4: Summer temperatures as the primary driver I would like to see a bit more detail on the physical flood generating mechanisms. From the discussion across pages 23 and 24, it follows that warmer winter air temperatures reduce annual snow storage and, in turn, the magnitude of the spring melt. But I note July temperature is used as the primary meteorological proxy (Figures 17 and 18 and associated text) and I can't figure out why summer temperature is more important than winter or spring temperature. I would have thought winter temperature would dictate snow volumes and spring temperature would influence rate of melting. I may well have misunderstood but, given this is a fundamental aspect of the interpretation, I suggest modifying the text – and reporting a comparison with winter and/or spring temperatures, if appropriate reconstructions are available - to ensure the reader can follow the process linkages at play. Similarly, Page 23 Line 28 also mentions the importance of winter precipitation. Does a regional precipitation reconstruction exist? I'm not doubting the authors' interpretation but I found myself wondering about the role of other drivers while reading this section so there is scope to tighten up the narrative and analysis here, in my opinion.

Author's response

We agree with the summary of flood generating mechanisms given by the reviewer. What we see from the flood events in the current climate is

- The flood seasonality in Fig 1 shows that the main flood season lasts from May to June which is locally known as the snow melt season. There are a few floods in the autumn season when periods of sustained rain are the most important flood generating process.
- Investigations of recent large flood events suggest that the key process that generate the largest floods are:
 - Large amounts of snow over large areas available for snow melt. This require high winter precipitation and preferentially low winter temperatures. Several studies indicate a link between snow accumulation and snow melt flood peak/volume in Scandinavia (e.g. Olsson et al, 2018)
 - A cold spring followed by a sudden increase in temperature typically result in high melt rates. Note that the variability and sequence of temperature is important.
 - Large amounts of widespread precipitation combined with snow melt. This factor can be related to spring / summer precipitation.
 - The largest flood in 1789 is not typical for these conditions since it happened in late July in 1789 and intense rain over several days provided the main bulk of the flood water. Snow melt from high altitude areas certainly also contributed, but most likely not to the same extent as for instance the large flood that occurred in 1995 (referred to as 'Vesle-Ofsen')

- Our challenge is to relate these conditions to climatic variables. We speculate that the following climate conditions can enhance floods and boost the flood frequency:
 - high winter precipitation (more snow will be accumulated throughout the season and also build up perennial snowfields in high mountain areas)
 - high summer precipitation (especially when it occurs early in the season as such combines with melting of snow)
 - cold winter and spring temperatures (by pushing back the snow melting well into the summer season the probability of a sudden, substantial raise in temperatures can enhance the potential melting considerably, typically going from under 10 °C to over 20 °C.)

Climate change impacts on floods in Norway is examined in detail by Lawrence (2020), and for the catchment studied here, a decrease in flood magnitude is to be expected. This is in agreement with what paleodata suggests (Støren & Paasche, 2014).

Within Norway there are, however, a variable response of flood magnitudes in snow-dominated catchments and Lawrence (2020) suggests that this reflects the competing effects of increasing winter precipitation and temperature. This anticipated change can lead to either an increase or a decrease in winter snow storage, and/or to an increase in rain-on-snow events throughout the winter half year, depending on the latitude and the elevation of the catchment.

An increase in temperature will also lead to a shift in flood seasonality and flood generating processes (Vormoor et al, 2015, 2016). For Elverum we might expect more frequent autumn floods and less frequent and smaller spring floods.

When it comes to discussing the flood generating mechanisms during the Holocene, we have chosen to compare our results (in fig. 18) with mean reconstructed mean July temperature (Velle et al 2010), and a high-resolution glacier reconstruction (Kvisvik et al 2015) from the mountain areas in the upper Glomma catchment as well as a flood index (Støren et al., 2012) denoting the relative distribution of Holocene floods in Southern Norway. Indeed, comparison to winter, spring and autumn temperature and precipitation reconstruction would have been preferable, but as the reviewer also recognize, there is presently a lack of appropriate climate reconstructions available. We use the plotted paleo-reconstructions to discuss the relative influence of changes in summer temperature, but also winter precipitation. We also utilize the flood index (Støren et al 2012) to briefly discuss the effect of changing atmospheric circulation distributing the winter precipitation e.g. causing a likely decrease in winter precipitation c. 2000-1000 cal. yr BP possibly explain the absence of floods recorded for this time interval (page 24 and 25).

We argue, however that summer temperature is highly correlated to winter temperature that can be considered as the main driver of Holocene flood frequencies in the Glomma catchment based on the observed variability both on instrumental and paleo-timescale. The explanation is likely to be linked to lower winter temperatures causing a higher potential for snow melt floods. In such a large catchment, with abundant perennial snow field in the mountains, and the potential for buildup of snowpack over several years, any changes in the flood frequency is deemed to be of regional nature. Consequently, it seems plausible that the effect of raising the 0-isotherm to a higher altitude, the effect of a warmer climate, will significantly change the potential storage of snow and thus flood frequency (see also Støren & Paasche, 2014).

Author's changes in manuscript

We have modified section 5.2 in the discussion chapter. (Pag 24 Line 35 –Page 25 Line 26)

Comment from the referee

Figure 3: do the authors have a photo or aerial/satellite imagery of the bifurcation inflow zone? I am intrigued but I am struggling to visualise what this looks like on the ground. Is there a dry channel or other morphological evidence to indicate this reverse flow occurs on occasion?

We do have good aerial photos of the bifurcation inflow zone. A photo will be included in fig. 3.

Author's response

From the photos one can see the following:

- At Vingersjøen, unambiguous morphological evidence reveal that reverse flow occurs. Especially, since the river that flows out of the lake has actually an inflow delta. The size of this delta has also increased in size.
- For the flow path from Tavern to Flyginnsjøen, there is little geomorphological evidence. The area with intermittent flows is forested or grassland, and the forest cover has increased somewhat the recent years. The most clear evidence are road bridges that has been built across these occasional streams.

Author's changes in manuscript.

We have modified Figure 3 by adding two areal photos of the area close to Kongsvinger (Page 6).

Comment from the referee

Figure 4 and 5: Figure 4 suggests the 'normal-flow' inlet to Flyginnsjøen is in the same corner but not in exactly the same place as the inflow under flood conditions, whereas Figure 5 lists only one inlet. I recognise this will have minimal effect but worth clarifying this morphology.

Author's response

Figure 4 ad 5: The two inlets into Flyginnsjøen enter the lake at the northern shore and are separated by approximately 30 meters. Note that there is not a delta where Vrangselva enters Flyginnsjøen, indicating that the background sediment influx is low.

Author's changes in manuscript

We have added this information in the text and in the captions of Figure 4 and 5. We have modified Figure 5 to show the two inlets into Flyginnsjøen (Page 5 Line 29, Page 6 Line 1 and Page 7).

Comment from the referee

The sequence of maps are a bit difficult to follow. For example, it's unclear whether Kongsvinger is a town. Perhaps the inset map in Figure 3 that has one red dot and the boundary of Norway could instead zoom in on a slightly larger area such that Elverum is also visible? Similarly, the locations

of the lakes, gauging stations, flood stones, towns and other features mentioned in the text are spread across 3, 4, 5 and 7 and I found myself having to flick back and forth between them.

Author's response

Kongsvinger is a town! At least after Norwegian standards. We agree that the sequence of maps is a little difficult to follow. A major challenge is that the Elverum-site for streamflow data and the paleodata at Kongsvinger are located 80 km apart, which is why we think it useful to provide an overview map in Figure 1, detailed maps for the paleo-data in Figures 3 and 4, and detailed map for the historical data in Figure 7. We will give an effort to present details and names in the correct order to simplify the reading of the manuscript, and in Figure 3 we will follow the suggestion to make an zoom in on a smaller area such that Elverum is also visible in the inset map in the upper right corner.

Author's changes in manuscript.

We have modified Figure 3 by zoom in on a smaller area so that Elverum is visible in the inset map in the upper right corner. We have also added one name that is used in the text (Vrangselsva) , and two areal photos of the area close to Kongsvinger (Page 6). We have also changed Figure 7 and the text and use the name 'Klokkefossen' for the location of one the flood stones (Page 10).

Comment from the referee

Figure 6: Given its use as a threshold, it would be worth labelling the 1967 flood in Figure 6

Author's response ‘

The 1967 flood is now labelled in Figure 6

Author's changes in manuscript.

We have modified Figure 6 including the threshold, added the discharge for the threshold and the length of the historical period. All details are explained in the figure caption. (Page 8)

Comment from the referee

Figures 14 and 15: I suggest the authors provide much more context and technical detail in the captions for Figure 14 and 15. I recognise these procedures are explored in the main text but, given their importance to the overall narrative, I think it would be really useful to present ample detail such that both figures can be interpreted on a standalone basis.

Author's response ‘

We agree

Author's changes in manuscript.

We have added more details in the figure captions in Figs. 14 and 15. such that both figures can be interpreted on a standalone basis. (Page 21 and 22)

Comment from the referee

Table 3: It took me a while to figure out the source of the pairs of correlation coefficients and why some were missing. I understand why the authors have presented the data in this way and it is probably fine to do so with some additional explanation. This might be resolved by writing in the

table caption which parameters were measured on which core and also being more explicit on which way round the numbers are reported. Or maybe report the coefficients for one of the cores entirely in italics?

Author's response

We have clarified the presentation of Table 3 by adding additional information to the caption and use typographic effects to highlight which correlations are from which core.

Author's changes in manuscript.

We have change Table 3 accordingly. (Page 16)

Minor comments

Comment from the referee

Section 3.3.1: given the broad audience of the journal, I question whether all readers will be aware of the reasoning behind using and integrating two cores (and indeed two types of corer).

Author's response

We agree and have add a few sentences explaining the reasoning for using and integrating two cores.

Author's changes in manuscript.

We have modified section 3.3.1 (Page 11, Line 14-17)

Comment from the referee

Page 11, line 27: the authors state they used a 9-month window in the peak detection algorithm. I like this approach as a way of considering event sequencing but what is the hydrometeorological basis for the 9-month window?

Author's response

First one clarification: In section 3.3.1 the 9 months refer to the minimum time lag between two succeeding flood events, it is not the size of the time window used in the flood detection algorithm. The hydrometeorological basis for choosing a 9-month time lag is that in this catchment there is, on average, one major flood event per year. This typically occurs in May/June. Only rarely do we observe large flood events during autumn. Consequently, we expect to detect only one major flood event per year. For locations with more frequent floods, a smaller time window could be more appropriate.

Author's changes in manuscript.

Se section 3.3.1 page 12 line 11-15 in the revised manuscript

Comment from the referee

Page 13, line 33: I suggest the authors report a range of layer thicknesses rather than stating “mm scale”.

Author's response

The term “mm scale” is meant as a descriptive term rather than a measure of precise thickness. Given the peak detection algorithm-approach used to recognize flood deposits in the sediment stratigraphy, we have not measured the thickness of all flood layers. This is not a trivial task, since the start and stop of a deposit can be gradual and the signal to noise ratio increase when values are low. We prefer to keep the term “mm-scale” and avoid defining start and stop of individual flood deposits.

Author's changes in manuscript.

None

Comment from the referee

Page 19, Line 11: Judging by eye, there is a more prominent step in flood occurrence rate at 700 yr BP rather than 600 yr BP?

Author's response

Thanks for pointing this out. We agree that there is a more prominent step in flood occurrence rate at 700 yr BP rather than 600 yr BP, and will change the text accordingly.

Author's changes in manuscript.

We have changed section 4.2 (Page 20, line 12)

Comment from the referee

Page 19, Lines 13-14: I find the assertion that “high flood frequency in the 18th century is also recorded in the historical flood data (Fig. 6)” to be unconvincing. There are very few data points prior to the 18th century (one?). As long as the authors can be confident the 15th and 18th-century peaks are not triggered by anthropogenic landscape modification, then the sediment record speaks for itself.

Author's response

We agree that the comment “*high flood frequency in the 18th century is also recorded in the historical flood data (Fig. 6)*” is speculative and we will delete it.

Author's changes in manuscript.

We have changed section 4.2 (Page 20, lines 14-15)

Comment from the referee

Page 20, Lines 18-20: I found it difficult to follow the sequence of different approaches applied in Section 4.3. In particular, which is “case ii above” (Line 18) and which is “case iii” (Line 19)?

Author's response

We will clarify the different approaches applied in section 4.3 when the paleoflood information is included in the flood frequency analysis.

-

Author's changes in manuscript.

We have modified section 4.3 and added table 6 to clarify the different approaches. (Page 21 and 22)

References

Kvisvik, B. C., Paasche, Ø. and Dahl, S. O.: Holocene cirque glacier activity in Rondane, southern Norway, *Geomorphology*, 11 246, 433–444, doi:10.1016/j.geomorph.2015.06.046, 2015.

Lawrence, D.: Uncertainty introduced by flood frequency analysis in projections for changes in flood magnitudes under a future climate in Norway, *Journal of Hydrology: Regional Studies*, 28, doi: 10.1016/j.ejrh.2020.100675, 2020

Olsson, J., Uvo, C.B., Foster, K., Yang, W. Technical Note: Initial assessment of a multi-method approach to spring-flood forecasting in Sweden. *Hydrol.Earth Syst.Sci* 20, 1-9, 2016

Støren, E. N., Kolstad, E. W. and Paasche, Ø.: Linking past flood frequencies in Norway to regional atmospheric circulation anomalies, *Journal of Quaternary Science*, 27(1), 71–80, doi:10.1002/jqs.1520, 2012.

Støren, E. N. and Paasche, Ø.: Scandinavian floods: From past observations to future trends, *Global and Planetary Change*, 36 113, 34–43, doi:10.1016/j.gloplacha.2013.12.002, 2014.

Støren, E. W. N., Paasche, Ø., Hirt, A. M. and Kumari, M.: Magnetic and geochemical signatures of flood layers in a lake system, *Geochemistry, Geophysics, Geosystems*, 17(10), 4236–4253, doi:10.1002/2016GC006540, 2016.

Velle, G., Bjune, A. E., Larsen, J. and Birks, H. J. B.: Holocene climate and environmental history of Brurskardstjøerni, a lake in the catchment of Øvre Heimdalsvatn, south-central Norway, *Hydrobiologia*, 642(1), 13–34, doi:10.1007/s10750-010-0153-7, 2010

Vormoor, K., Lawrence, D., Heistermann, M., Bronstert, A., Climate change impacts on the seasonality and generation processes of floods – projections and uncertainties for catchments with mixed snowmelt/rainfall regimes. *Hydrol. Earth Syst. Sci.* 19, 913–931. 2015

Vormoor, K., Lawrence, D., Schlichting, L., Wilson, D., Wong, W.K., Evidence for changes in the magnitude and frequency of observed rainfall vs. Snowmelt driven floods in Norway. *J. Hydrol.* 538, 33–48, 2016

Wilhelm, B., Ballesteros Canovas, J. A., Corella Aznar, J. P., Kämpf, L., Swierczynski, T., Stoffel, M., Støren, E. and Toonen, W.: Recent advances in paleoflood hydrology: From new archives to data compilation and analysis, *Water Security*, 1–8, doi: 10.1016/j.wasec.2018.07.001, 2018.

New flood frequency estimates for the largest river in Norway based on the combination of short and long time series

Kolbjørn Engeland¹, Anna Aano^{1,2}, Ida Steffensen³, Eivind Støren^{3,4}, Øyvind Paasche^{4,5}

¹The Norwegian Water Resources and Energy Directorate, Oslo, Norway

²Department of Geosciences, University of Oslo, Norway

³Department of Earth Science, University of Bergen, Norway

⁴Bjerknes Centre for Climate Research, Bergen, Norway

⁵NORCE Climate, Bergen, Norway

Correspondence to: Kolbjørn Engeland (koe@nve.no)

Abstract. The Glomma river is the largest in Norway with a catchment area of 154 450 km². People living near the shores of this river are frequently exposed to destructive floods that impair local cities and communities. Unfortunately, design flood predictions are hampered by uncertainty since the standard flood records are much shorter than the requested return period and also the climate is expected to change in the coming decades. Here we combine systematic- historical and paleo-information in an effort to improve flood frequency analysis and better understand potential linkages to both climate and non-climatic forcing. Specifically, we (i) compile historical flood data from the existing literature, (ii) produce high resolution X-ray fluorescence (XRF), Magnetic Susceptibility (MS) and Computed Tomography (CT) scanning data from a sediment core covering the last 10 300 years, and (iii) integrate these data sets in order to better estimate design floods and assess non-stationarities. Based on observations from Lake Flyginnsjøen, receiving sediments from Glomma only when it reaches a certain threshold, we can estimate flood frequency in a moving window of 50 years across millennia revealing that past flood frequency is non-stationary on different time scales. We observe that periods with increased flood activity (4000-2000 years ago and <1000 years ago) corresponds broadly to intervals with lower than average summer temperatures and glacier growth whereas intervals with higher than average summer temperatures and receding glaciers overlap with periods of reduced number of floods (10 000 to 4000 years ago and 2200 to 1000 years ago). The flood frequency shows significant non-stationarities within periods having increased flood activity as was the case for the 18th century, including the AD 1789 ('Stor-Ofsen') flood being the largest on record for the last 10 300 years at this site. Using the identified non-stationarities in the paleoflood record allowed us to estimate non-stationary design floods. In particular, we found that the design flood was 23% higher during the 18th century than today and that long-term trends in flood variability are intrinsically linked to the availability of snow in late spring linking climate change to adjustments in flood frequency.

Keywords: flood, lakes, extremes, paleofloods, Norway, non-stationarity.

1 Introduction

Floods are among the most widespread natural hazards on Earth. The impacts, destruction and costs associated with hazardous floods are ~~increasing~~ increasing in concert with climate change and increase of economic values within areas susceptible to floods, a the trend in flood risk that is area tendency most likely to strengthen in the decades to come (e.g. Alfieri et al., 2017; Hirabayashi et al., 2013; IPCC, 2012). In Europe, spatial flood patterns are changing both in terms of timing and magnitude (Blöschl et al., 2017, 2019) challenging us to examine new ways to interlink not only different types of data, but also flood information on different time scales. Earlier studies have shown that uncertainties can be reduced if, for instance, historical data are included in estimation of floods with long return periods (e.g. Brázdil et al., 2006a; Engeland et al., 2018; Macdonald et al., 2014; Payraastre et al., 2011; Schendel and Thongwichian, 2017; Stedinger and Cohn, 1986; Viglione et al., 2013). Here we seek to extend the possibility of using historical data by including time series of reconstructed floods based on lake sediment archives which can retain imprint of past flood activity (Gilli et al., 2013; Schillereff et al., 2014; Wilhelm et al., 2018). The ultimate goals of this exercise are to (i) reduce uncertainty associated with flood prediction and (ii) provide additional insight to flood variability on longer time scales, and thereby improve our understanding of how climate change impacts floods.

In many European countries, flood mitigation measures aim to reduce the exposure and vulnerability of the society to floods. Examples of such measures can include reservoirs, flood safe infrastructure, and land-use planning in flood-exposed areas. These mitigation measures require estimates of design floods, i.e. the flood size (typically given in m^3/s) for a specified annual exceedance probability (AEP) or return period (RP). The required design AEP or RP depends on the impact of a flood. The Norwegian building regulations (TEK17, 2018) exemplifies this. They require that ~~that~~ buildings of particular societal value such as hospitals should be able to resist or be protected from at least a 1,000-year flood whereas normal settlements should withstand 200-year flood and storage facilities at least a 20-year flood. Design flood estimates are commonly based on analysis of the frequency and magnitudes of observed floods using measurements derived from a streamflow gauging station. Recall that for many applications, estimates of 200- up to 1000-year floods are required (see Lovdata, (2010) and TEK17, (2018) for regulations in Norway). This is not a trivial task for at least two reasons. Firstly, we have limited amount of data and the estimation uncertainty for a 1000-year flood is large with only 50-100 years of data. Secondly, we plan for the future (i.e. for the life time of a construction), but in many cases it can be necessary to account for non-stationarities in floods caused by past as well as anticipated future changes in climate.

Both challenges can be addressed by using data covering longer time periods including historical data (e.g. Benson, 1950; Brázdil et al., 2006b; Macdonald et al., 2014; Schendel and Thongwichian, 2017; Viglione et al., 2013) and/or paleoflood data (e.g. Benito and O'Connor, 2013). The fact that sediment deposits can be unambiguous evidence of past floods is documented in many studies since 1880 AD (Bretz, 1929; Dana, 1882; Tarr, 1892), and an early example of how to estimate discharge associated with giant paleofloods can be found in Baker (1973) whereas paleoflood hydrology as a concept and terminology was first introduced by Kochel and Baker (1982).

In order to include information about past floods in flood frequency analysis, it is necessary to estimate the flood sizes in m^3/s . A successful approach for assessing the stage and the volumes for paleofloods is to use slack-water deposits along river canyons (e.g. Baker, 1987, 2008; Benito and O'Connor, 2013; Benito and Thorndycraft, 2005). Following this approach, water level during floods can be deduced from the elevation of the deposits enabling hydraulic models to estimate flood volumes for specific events. During the recent 20 years, lacustrine sediments has proven to be another reliable source of paleofloods (Gilli et al., 2013; Schillereff et al., 2014; Wilhelm et al., 2018). Sediment cores retrieved from lakes that periodically receive sediments delivered by floods can be used to extend local hydrological time series spanning thousands of years. Since lake sediment archives for the most are continuous records, they can complete the snapshot information provided by flood terraces still present in the landscape or anecdotal information about historical floods.

Lakes fit for using lacustrine sediments to analyze flood frequencies are typically found where (i) flood sediments are preserved at the bottom of lakes (ii) there is a detectable on/off signal for sediments left by floods, and (iii) a distinct contrast

1 between flood deposits and regular background sedimentation (Gilli et al., 2013). Detection of flood layers in the cores can be
2 based on X-ray fluorescence (XRF) scanning (e.g. Czymzik et al., 2013; Støren et al., 2016) magnetic susceptibility (MS)
3 measurements (e.g. Støren et al., 2010), computed tomography (CT) scanning (e.g. Støren et al., 2010), or spectral reflectance
4 and color imaging (Debret et al., 2010).

5 There are multiple sources for historical flood data ~~including (i) annals, chronicles, memory books and memoirs; (ii)~~
6 ~~weather diaries; (iii) correspondence (letters); (iv) special prints; (v) official economic and administrative records; (vi)~~
7 ~~newspapers and journals; (vii) sources of a religious nature; (viii) chronogramme; (ix) early scientific papers, compilations~~
8 ~~and communications; (x) stall keepers' and market songs; (xi) pictorial documentation; and (xii) epigraphic sources (e.g.~~
9 ~~Brázdil et al., 2012).~~ And Depositories of historical flood data are listed can be found in Brázdil et al. (2006a) and Kjeldsen
10 et al. (2014). An overview over historical floods in Norway is available in Roald (2013). For quantitative analyses, it is
11 nonetheless necessary to find evidence of historical flood stages, e.g. from flood stones or flood marks, and estimate flood
12 discharge based on hydraulic calculations (Benito et al., 2015).

13 Systematic measurements of floods date back to the Common Era (CE) 1870. Historical flood information in Norway
14 is often available back to the 17th century, there is, however, scattered information on earlier floods including one that occurred
15 in the 1340s. This is different from paleoflood data in Norway which typically cover the Holocene period (11700 years) and
16 extends all the way until present day. The difference in time periods covered by diverse data sources on past flooding highlights
17 the potential of using historical- and paleo flood data to both reduce estimation uncertainty of design floods with long return
18 periods and to assess non-stationarities in floods.

19 The paleo- and historical flood information can be used – in combination with systematic data – to estimate design
20 floods (see e.g. Engeland et al., 2018; Kjeldsen et al., 2014; Stedinger and Cohn, 1986). To include the paleo- and historical
21 information in flood frequency analysis, we also need to know all floods exceeding a fixed threshold during a specified time
22 interval. Several studies demonstrate that, given that the fixed threshold is high enough, it is adequate to know the number of
23 floods exceeding this threshold in order to improve flood quantile estimates (Engeland et al., 2018; Martins and Stedinger,
24 2001; Payraastre et al., 2011; Stedinger and Cohn, 1986). A Bayesian approach to flood frequency analysis with historical- and
25 paleodata sources was introduced by Stedinger and Cohn (1986) and Gaál et al. (2010). This approach allows, in a flexible
26 way, the introduction of multiple fixed thresholds and data sources, and is therefore well suited for combining systematic-
27 historical and paleo- data in a joint flood frequency analysis.

28 When we predict flood frequency for the future, the standard assumption is stationarity or put differently: it's assumed
29 that the period with instrumental data is representative for the future. In many cases, when the analysis is based on flood data
30 from a streamflow gauging station covering a limited period, it is a robust assumption (Serinaldi and Kilsby, 2015). However,
31 in the face of expected changes in climate, it is useful to take into account the risk for floods in the future (Hanssen-Bauer, ~~I.~~
32 ~~Førland, E. J. Haddeland~~ et al., 2017; Lawrence, 2020; Paasche and Støren, 2014). For Norway, tailored guidelines for adaption
33 to future flood risk are provided by the Norwegian Center for Climate Services (<https://klimaservicesenter.no/>) based on
34 results from climate projection studies (Lawrence, 2020). A current practice is to use flood inundation maps where estimated
35 future flood levels for specific return periods are shown (e.g. NVE flood zone maps, 2020;- Orvedal and Peereboom, 2014).
36 Such maps are commonly used in land-use planning.

37 Since the historical- and paleodata covers much longer time periods than streamflow data, they can be an excellent
38 source for non-stationarity in actual flood sizes and the underlying flood generating processes. One approach is to link the
39 frequency of floods to the underlying climatic drivers (e.g. mean temperature, precipitation and large-scale circulation patterns
40 (e.g. Gilli et al., 2013; Kjeldsen et al., 2014; Støren et al., 2012; Støren and Paasche, 2014). A major challenge when using
41 paleo- and historical flood information, is precisely to disentangle non-stationarity in climatic drivers from non-stationarities
42 caused by changes in land-use and/or the 'archiving processes' of the data. Changes in land-use can, for instance, be related to
43 farming practices and timber-logging. Changes in the archiving process might be caused by changes in the perception threshold

1 that depend on societal development (Kjeldsen et al., 2014; Macdonald and Sangster, 2017). Also changes in the river channel
2 might limit the possibility to estimate the magnitude of paleo- and historical floods (Brázdil et al., 2011).

3 The primary objective of this paper is to combine systematic- historical and paleo-information in a flood frequency
4 analysis in order to better understand and predict changes in flood frequency and magnitude for Norway's largest river,
5 Glomma. In particular we want to explore:

- 6 • Past variability in floods as reconstructed from lake sediment cores.
- 7 • Potential non-stationarity in our new paleoflood record and its potential connection to regional climate change.
- 8 • The added value of combining systematic-, historical-, and paleo-flood data when estimating flood quantiles.
- 9 • Potential non-stationarities in design floods.

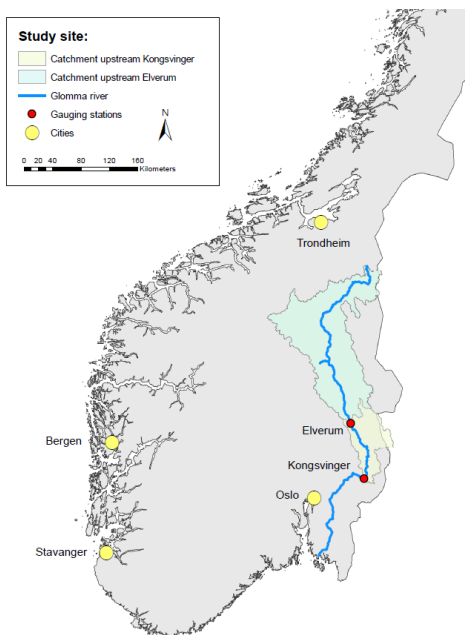
10 The unique contribution of this study is thus to combine three different information sources in an attempt to improve flood
11 frequency estimations and better understand the underlying mechanisms that cause significant changes in flood variability over
12 time.

13 2 Study area

14 2.1 Study catchment

15 The target site for this study is the city Elverum lying next to the river Glomma. ~~A gauging station having~~ station having an
16 upstream catchment area of 154 450 km² (Fig. 1) is located within the city. -The elevation in the catchment ranges from 180
17 masl at Elverum to 2178 masl at ~~the highest mountain Mt. Rondslettet in Rondane further north,~~ and is covered by forest (52
18 %), open areas above the timber line (27%), bogs (10 %), lakes (3%), and agricultural areas (2%). Only 0.13% is represented
19 by urban areas. The average annual precipitation is 580 mm with the summer months being the wettest. The annual average
20 temperature is -0.65 °C but the climate is continental. January has the coldest month with -11.2 °C whereas July is the warmest
21 with 10 °C. The low winter temperatures result in a considerable seasonal snow cover which has a direct impact on the
22 streamflow. Minimum flows are observed during winter (December – April) whereas the highest flows take place during the
23 snow melt season (May – June), as shown in Fig. 2. The main flood season occurs during the snow melt season (May – June)
24 with the rare exception of a few minor floods that arrive during the autumn season due to long duration intense rainfall.

25

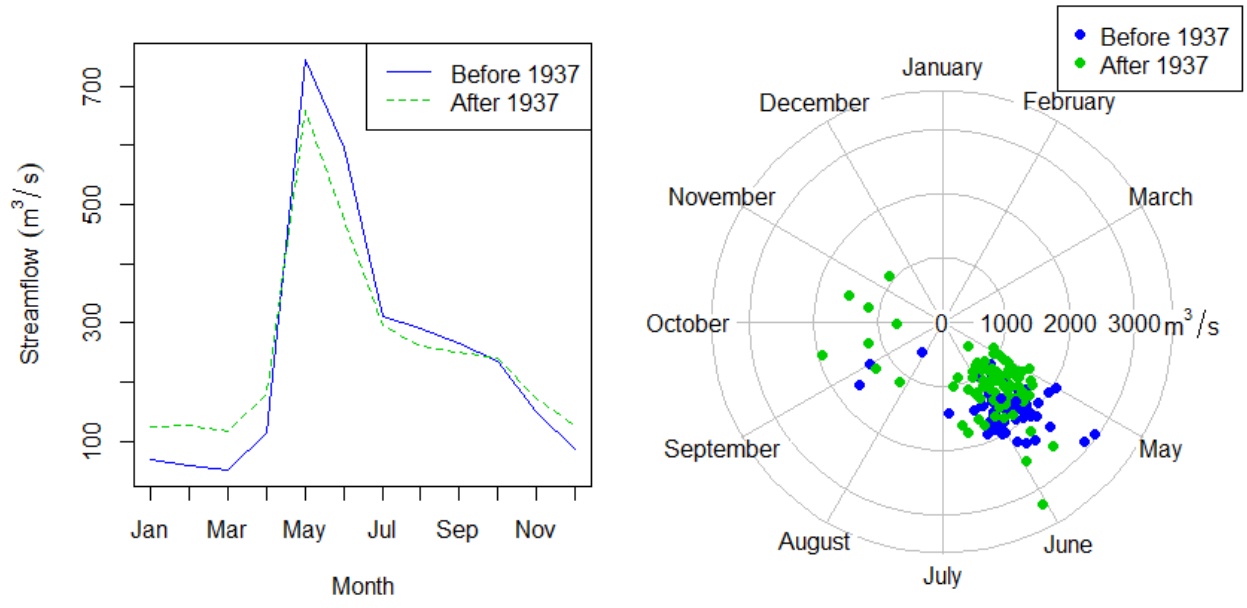


26

27 Figure 1: The location of the streamflow gauging station at Elverum used for flood frequency analysis, and the site for paleodata
28 collection close to Kongsvinger city.

1
2
3
4
5
6
7
8
9
10

The catchment has several hydropower reservoirs with a total regulation capacity presently around 10% of the average annual runoff. The first reservoir was built in 1913, and since 1937 this and other reservoirs have resulted in decreased flood sizes (Pettersson, 2000). The monthly flows during winter has increased and most flood peaks have decreased after 1937 (Fig. 2). The catchment has undergone noteworthy land-use changes during the last 400 years. In the 17-19th century, the forest areas were reduced due to mining, timber export and farming practices. Since the beginning of the 20th century, the forest covered areas have increased slightly whereas the timber volume has increased substantially mainly due to farming and forestry practices e.g. reduced grassing of domestic livestock and forestation, (Grønlund et al., 1999).



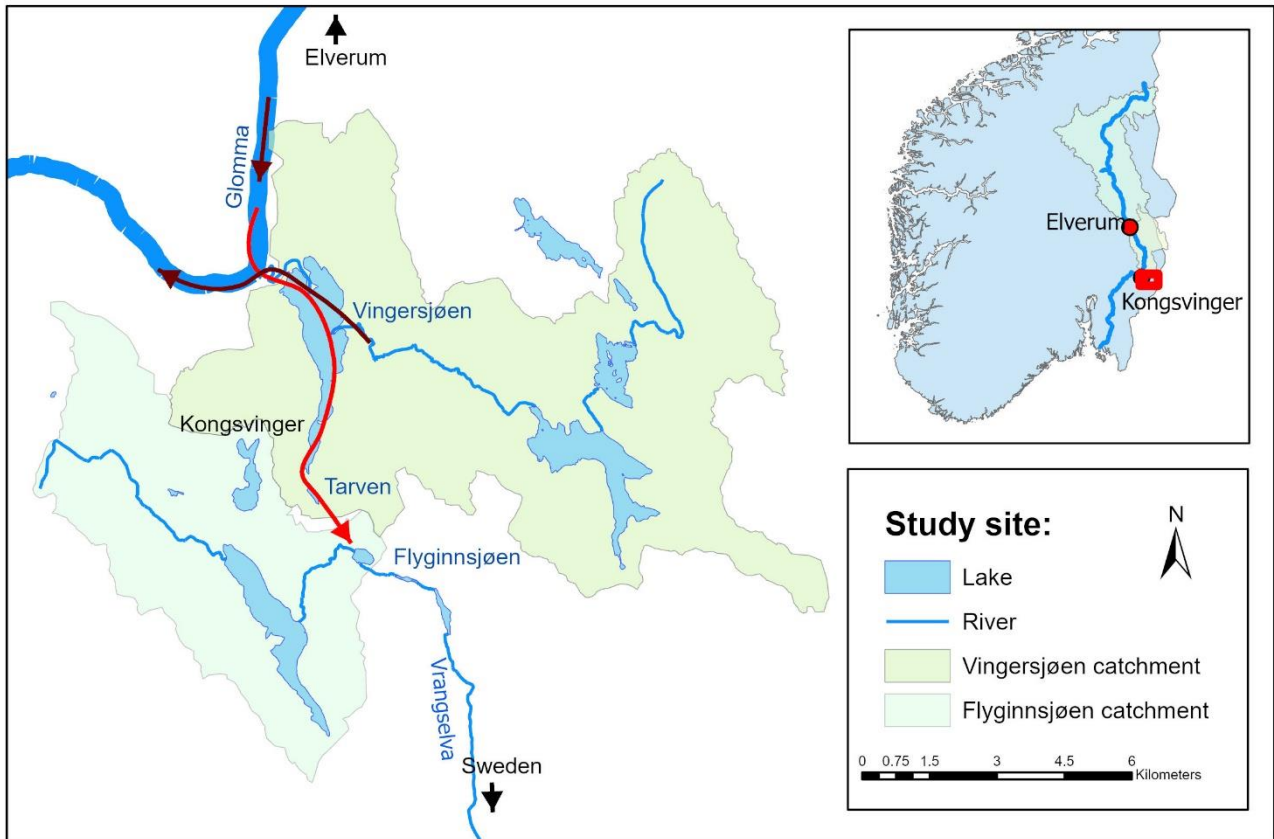
11
12
13
14
15
16

Figure 2: Seasonality of Glomma's monthly streamflow (left) and annual maximum floods (right) at Elverum. The dampening of floods after 1937 is explained by up-stream dam-building.

2.2 Study site for paleodata

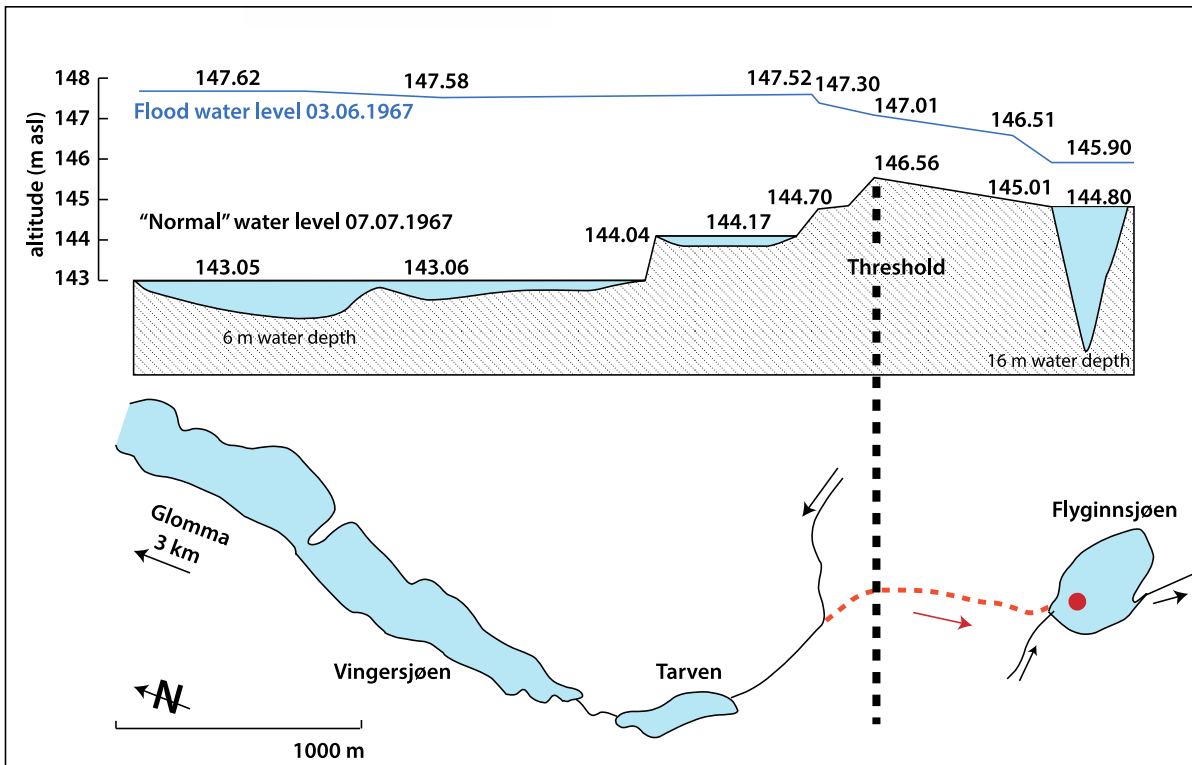
To establish a flood record covering most of the Holocene (<11 700 years, Walker et al. (2009)), two sediment cores were retrieved at 16 m water depth from Flyginnsjøen (UTM: 33V 0337459 6670202) located close to Kongsvinger, around 80 km south of Elverum as the crow flies (Fig. 1). A detailed map of the study area is shown in Fig.3 and conceptual model of the lakes involved, flood water levels, thresholds and flood pathways are shown in Fig. 4. During normal conditions, water flows from FavernTarven and Vingersjøen (catchment area 72.0 km²) into Glomma. When the streamflow in Glomma exceeds 1500 m³/s, the flow direction reverses, and around 1-2 % of the water flows from Glomma and over to Vingersjøen and further into FavernTarven. Flyginnsjøen, leaves the Glomma catchments and follows the river Vrangselva across the border to Sweden (Pettersson, 2001). These bifurcation events enable flood water from Glomma to reach Flyginnsjøen where part of the suspended sediment load is deposited. This is in stark contrast to 'normal conditions' for the lake, when the minerogenic sediment delivery is marginal compared to the organic material, as outlined below. The repeated increase in discharge during floods, remobilize readily available sediments – originating mainly from the last deglaciation – and allow for the subsequent deposition of fine-grained minerogenic material. Bathymetric map of Lake Flyginnsjøen and the coring sites which were chosen at the deepest part of the lake, close to the inlet is shown in Fig. 5. Note that the inlet during bifurcation events is only

1 [around 30 meters away from the permanent inlet](#). For addition details about the study site, and its surroundings, see the master
2 theses by Aano (2017), Follestad (2014), and Steffensen (2014).



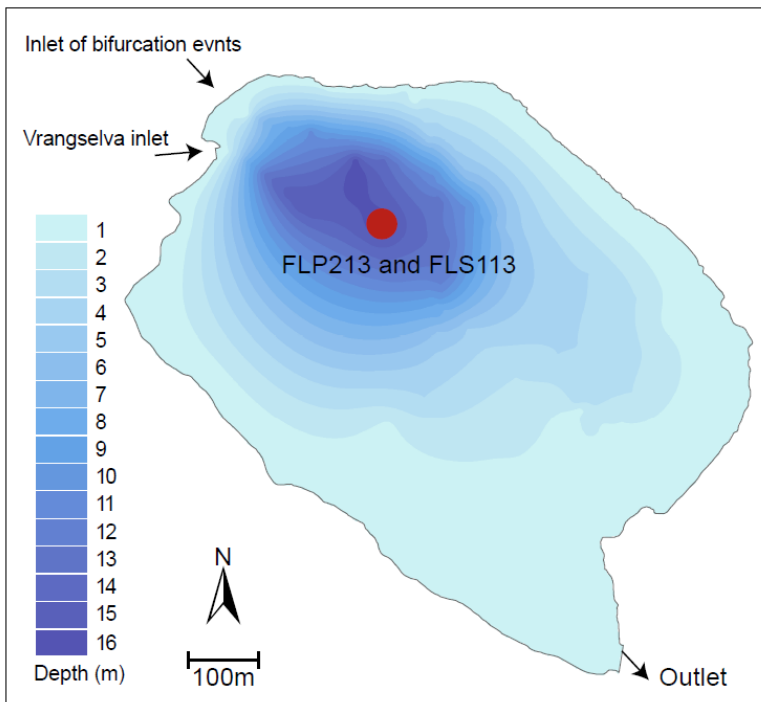
Areal photo: © Norwegian Mapping Authority, Geovekst and the municipalities, Oslo-Østlandet 2016

3
4 Figure 3: Study site for the paleodata. [Map](#): The sediment cores were extracted from lake Flyginnsjøen. The green arrows
5 indicate the flow direction under normal conditions, whereas the [dark red](#) arrow shows the flow direction whenever there is a
6 flood that exceeds $1500 \text{ m}^3/\text{s}$ and bifurcation occurs. [Left areal photo](#): The river between Vingersjøen and Glomma. Under
7 [normal conditions](#) the water flows from Vingersjøen into Glomma. [Right areal photo](#): The flood path from Tarven to
8 [Flyginnsjøen](#) during bifurcation events is indicated with red dots. Areal photo: © Norwegian Mapping Authority, Geovekst
9 [and the municipalities, Oslo-Østlandet 2016](#).



1
 2 Figure 4: Schematic model of the lakes involved, flood water levels, thresholds and flood pathways (After Hegge, 1968).
 3 The example shows observed water level exceeding the threshold during the flood in 1967 (2533 m³/s), and the normal water
 4 level approx. one month after the flood event. The dotted red line and arrow show the bifurcation over the threshold, and the
 5 red point marks the coring site in Flyginnsjøen.

6 Note that the inlet during bifurcation events is only around 30 meters away from the permanent inlet.



8
 9 Figure 5. Bathymetric map of Lake Flyginnsjøen and the coring sites which were chosen at the deepest part of the lake, close
 10 to the inlet. Note that the inlet during bifurcation events is only around 30 meters away from the permanent inlet.

3 Data sources and Methodology

3.1 Systematic flood data

Annual maximum flood at Elverum (station number 2.604) for the period 1872–1936 was used for the flood frequency analysis. For this period, we assumed that the flood data were not significantly affected by river regulations (Pettersson, 2000). The mean annual flood for the period 1937–2019 is 1362 m³/s. A Wilcoxon test indicates that the difference in mean value is significant with a p-value < 0.01 for the zero-hypothesis (i.e. no difference in mean values between the two periods). The modern observations are shown in Fig. 6 together with the known historical floods as well as annual maxima daily floods from the period after 1937, when we observe a minor decrease in average flood size after 1937.

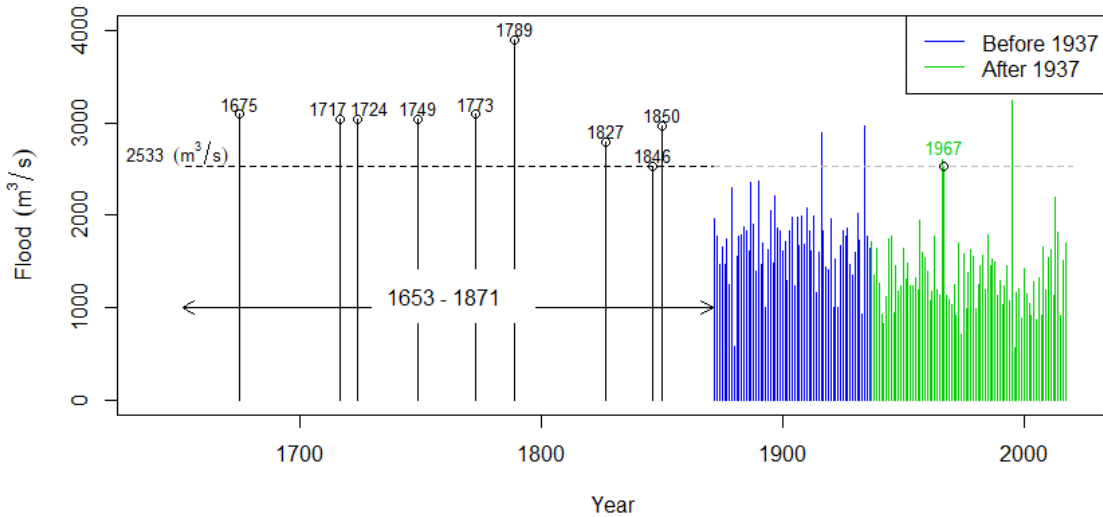


Figure 6: Systematic and historical flood data at Elverum. The systematic data from 1872 – 1936 were used for flood frequency analysis. After 1937, the floods are significantly affected/dampend by river regulations. The flood in 1967 reached 2533 m³/s and was used as a threshold for the historical floods. The period for historical floods lasted from 1653-1871. The CE 1789–AD flood known as *Stor-Ofsen* in Norway stand out in this record.

3.2 Historical flood data

Historical flood information back to 1675 is available as water levels marked at a flood stone in Elverum, located close to Klokkerfossen (‘fossen’ meaning waterfall) at the Norwegian Forest Museum in Elverum (Fig. 7 and Table 1-2). Table 1 lists the water levels and discharges for floods exceeding the 1967 flood are highlighted on the flood stone which was erected in 1968. The water levels were carved into the stone in 1969 based on recommendations from NVE (Hegge, 1969); the 1995 flood was added later. There is another flood stone nearby at Grindalen (also shown in Fig. 7). It was erected as early as in 1792 in order to remember the floods of 1773 and 1789, which were large indeed.

The flood stone at Grindalen is 2 km upstream the flood stone at Klokkerfossen with the streamflow gauging station at Elverum in the middle. A waterfall at Klokkerfossen is the controlling profile for the water levels at all three locations. Hegge (1969) developed relationships between water levels at the Elverum gauging station and the flood stone at KlokkerPrestfossen shown here in Table 1. The water levels at Elverum gauging stations were transformed to discharges by using the local rating curve, and thereby assuming which assumes that the river profile washas been relatively stable since CE 1675. In this study, we included all floods exceeding the observed 1967 flood peak at 2533 m³/s in the flood frequency analysis. By following this approach, we are confident that we only included information about all floods exceeding a specific flood level.

Table 2 summarizes the available historic information and important sources for these floods. The floods in 1675, 1717, and 1749 are all described in Finne-Grønn (1921) and Otnes (1982) whereas information for the flood mark in 1724 is not found in any written source. Detailed information about water levels for floods prior to 1773 were estimated in the absence

of historical data. The water levels in 1773, 1789, 1827 and 1846 are all engraved in the flood stone in Grinsdalen and employed here as a basis for calculating the water level at the Elverum gauging station and also for the flood stone at Klokkearfossen. Having said that, we still included all flood water levels listed in Hegge (1969). More information about historical flood of the Glomma River and at Elverum is provided by Finne-Grønn (1921), Otnes (1982), and Roald (2013). During the period 1675 to 1870, we see that 8 floods exceeded the observed 1967 flood peak at 2533 m³/s. The 18th century has a large number of floods at this location. All floods occurred in late May with the notable exception of *Stor-Ofsen* in 1789 which occurred in late July.

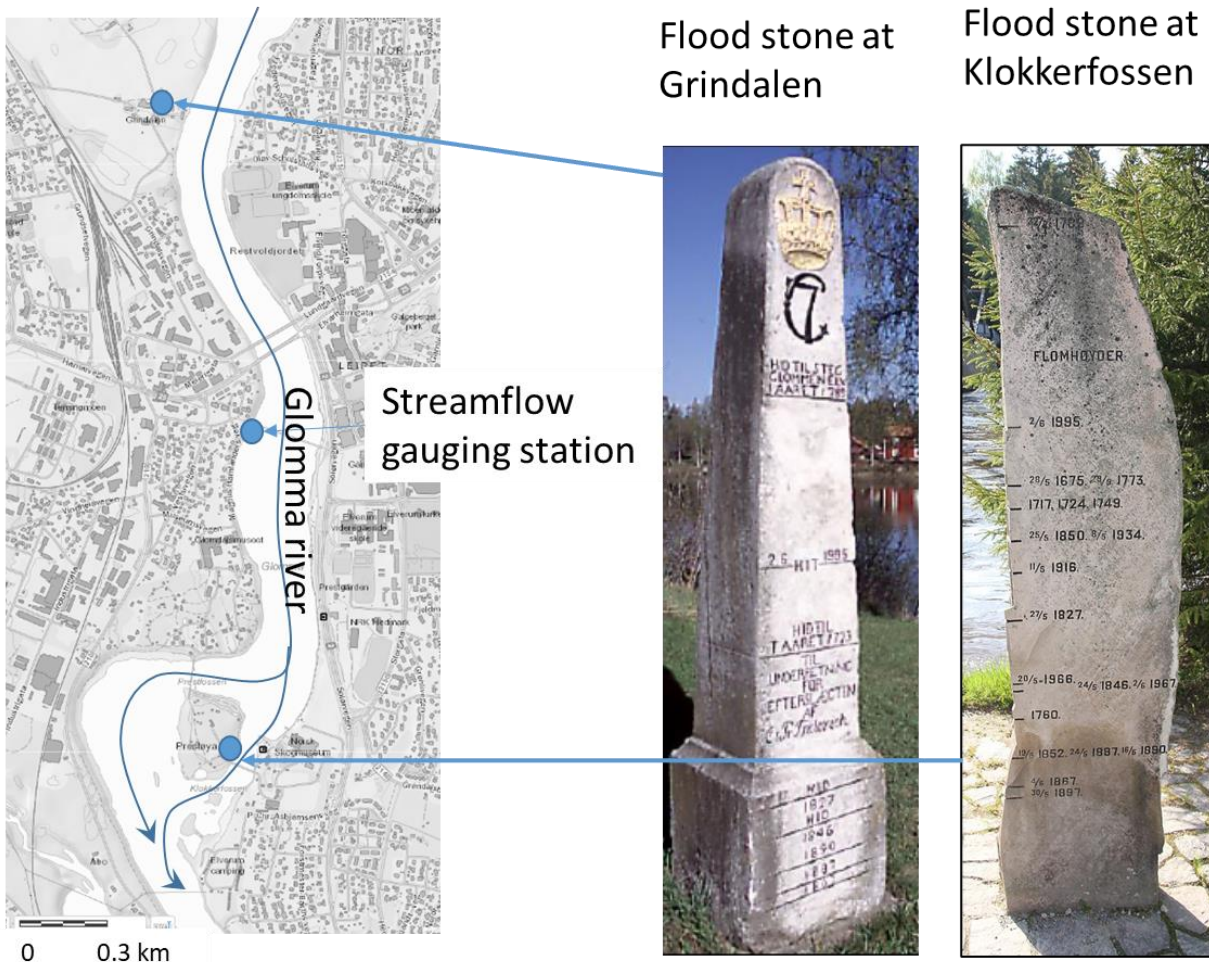
The largest historical flood in this region was *Stor-Ofsen* which took place in 22-23 July 1789 when peak discharge reached 3900 m³/s at Elverum (GLB, 1947) being only slightly smaller than our estimate (see Table 1). Numerous catchments in eastern Norway flooded at the time resulting in 61 fatalities, destruction of infrastructure, farms and crops. The economic losses were extraordinary and in the aftermath of the flood, around 1500 farms got tax reduction (Otnes, 1982).

Table 1: Water levels at Elverum gauging station and at the flood monument from Hegge (1969). The various streamflow peaks are constructed based on the rating curve at the gauging station 2.119 and rating curve period 1881-1970. The large floods in 1966, 1967 and 1995 were not used included in this study.

Date	Height – gauging station (m)	Height – flood monument (m)	Streamflow (m ³ /s) Peaks
28.05.1675	4.50	3.35	3141
24.05.1717	4.30	3.22	2963
17.21.1724	4.25	3.19	2919
24.05.1749	4.20	3.16	2875
30.05.1773	4.55	3.38	3187
22.07.1789	5.35	3.86	3944
27.05.1827	4.04	3.06	2736
24.05.1846	3.87	2.95	2592
25.05.1850	4.33	3.24	2989
11.05.1916	4.30	3.22	2892
08.05.1934	4.36	3.26	2963
20.05.1966	3.90	2.97	2600
02.06.1967	3.87	2.95	2533
02.06.1995	---	---	3238

Table 2 Information about large historical floods at Elverum.

Date	Information	Source
28.05.1675	Large flood in Elverum used as a reference for later floods.	Finne-Grønn (1921) Otnes (1982)
24.05.1717	The largest flood since 1675	Finne-Grønn (1921) Otnes(1982)
1724	No information found	
24.05.1749	Large amounts of snow during winter. The flood was smaller than in 1675 and similar to the floods in 1717 and 1724. The flood peaked around 12:00.	Finne-Grønn (1921) Kvernmoen and Kvernmoen(1921)
29-30.05.1773	Highest flood in man's memory and higher than in 1675. The whole village flooded. Marked at flood stone in Grindalen	Finne-Grønn (1921) Kvernmoen and Kvernmoen(1921)
22-24.07.1789	The flood peaked between 22:00 and 24:00 the whole village at Elverum destroyed. Marked at flood stone in Grindalen.	GLB (1947)
27.05.1827	2.5 alen (156 m) lower than 1789 and 0.5 alen (31.3 cm) lower than 1773. Almost the whole village was flooded. Marked at flood stone in Grindalen.	Otnes (1982)
26.05.1846	Marked at flood stone in Grindalen.	Roald (2013)
24-26.05.1850	Marked at flood stone in Grindalen.	Roald (2013)



2

3 Figure 7: Map on the left shows the locations of the flood stones and the gauging station at Elverum (left). Pictures to the right
 4 shows the flood monuments at Grindalen (middle, photo: N.R. Sælthun) and [Klokkerfossen](#) at the Norwegian forest museum
 5 (right, photo: Ø. Holmstad).

6

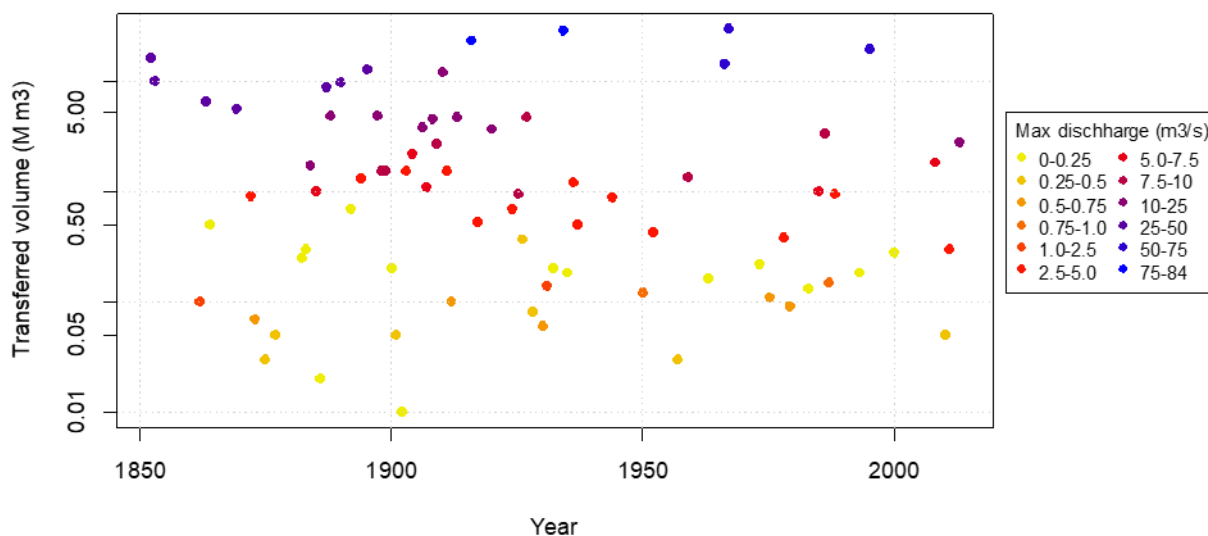
7 Prior to *Stor-Ofsen*, there was a substantial amount of snow in the mountains, deep soil frost, and rainfall that had
 8 saturated the soil. During the actual flood event, warm and humid air masses from the southeast were blocked by colder air
 9 masses in the north-west, resulting in high rainfall over the entire region. The rainfall intensity peaked on the 22 July. The
 10 flood started on 21 July in small brooks and culminated the following day (Østmoe, 1985). The main rivers at the bottom of
 11 the valleys rose to unprecedented levels and the flood was also accompanied by numerous landslides. The water levels of this
 12 flood are known from several markings cut into rocks, and many flood levels have later been transferred to monuments erected
 13 at locations near the major rivers (Engeland et al., 2018; Finne-Grønn, 1921; Otnes, 1982; Roald, 2013).

14

15 3.2.1 Bifurcation events

16 Descriptions of bifurcation events and lists of estimated flow volumes in Glomma at Kongsvinger are found in Aano (2017),
 17 Pettersson (2001), Hegge (1968), and Reusch (1903). From 1851 to 2013, 79 events in 77 different years were recorded. In
 18 1957 and 1987 there were bifurcation events both in the spring and in the autumn; 4 of the 79 events occurred during the
 19 autumn. For the interval between 1953-2013, the same period that is covered by FLS113, there were 22 bifurcation events.
 20 The transferred volume for the period 1851-2013 is presented in Fig. 8. The five years with the largest transferred volumes are
 21 1916, 1934 1966, 1967 and 1995 with corresponding peak floods at Elverum yielding 2892, 2963, 2600, 2533, and 3238 m³/s,
 22 respectively. Note that there is a strong statistical correlation (rsq=0.94) between transferred volume and the maximum

1 transferred discharge. In addition to actual discharge of the individual floods, the duration of each bifurcation event determines
 2 the total volume. The estimated peak bifurcation discharge in 1995 was substantially smaller than the estimate for 1916, despite
 3 the fact that the water level in Glomma was somewhat higher in 1995 (Pettersson, 2001). Possible explanations for this minor
 4 discrepancy are that increased vegetation and/or a local road bridge has reduced the capacity of the intermittent water course.
 5 The number of events has decreased since around 1930, mainly due to construction of hydropower reservoirs.
 6



7
 8 Figure 8: Transferred volume ($M \text{ m}^3/\text{s}$) and maximum discharge (m^3/s) indicated by color for bifurcation events at
 9 Kongsvinger. Estimates are obtained from Aano (2017), Pettersson (2001), Hegge (1968), and Reusch (1903).
 10

11 3.3 Paleohydrological flood data from lakes

12 3.3.1 Identification of sediment layers

13 Two sediment cores were retrieved from Flyginnsjøen in 2013 (see Sect. 2.2). Coring sites shown in Fig. 5 were selected were
 14 chosen at the deepest part of the lake based on a bathymetric survey of the lake using a Garmin Fishfinder echo sounder. and A
 15 516 cm long sediment cores were retrieved using a 110 mm diameter piston corer (FLP213) (Nesje, 1992). Since the piston
 16 corer may disturbs sediment layers in the upper 15-20 cm and an HTH gravity corer (FLS113) (Renberg and Hansson, 2008)
 17 was used to retrieve a 18 cm core of the youngest sediments. Samples of 1 cm^3 were extracted at 0.5 cm intervals from the
 18 sediment cores, dried overnight at $105 \text{ }^\circ\text{C}$, and weighed to measure dry-bulk density (DBD) (Blake and Hartge, 1986). The
 19 same samples were subsequently burned at 550°C to measure the weight loss-on-ignition (LOI) as an estimate of the organic
 20 matter content (Dean, 1974). Geochemical properties of the sediment cores were measured using a Cox Analytics ITRAX
 21 XRF core scanner at $200 \mu\text{m}$ resolution, running a Cr X-ray tube at 30 kV and 45mA for 10 sec. measurements at each step.
 22 XRF measurements were normalized against total scatter (incoherent and coherent) to reduce potential influence of water
 23 content. Images of the split core surface was also captured by the ITRAX core scanner, and 8-bit (255 values) Black & White
 24 (BW) values were obtained from a 75 pixel wide average along the length of the core at $200 \mu\text{m}$ resolution using Image J
 25 software. A ProCon Alpha Core Computed Tomography (CT) scanner running at 100 kV, 200 mA for 250 ms was used to
 26 generate 3D X-ray imagery of FLS113 with a voxel resolution of $80 \mu\text{m}$. CT data was reconstructed using ring-artefact and
 27 median filter in the Volex CT Offline software (ProCon X-ray gmbh), and visualized in Avizo Fire 9.1 (FEI) software. The
 28 CT data is given as 16-bit (65636 values) grayscale values, interpreted to indicate relative densities due to minimal
 29 photoelectric effect at 100 kV (Wellington and Vinegar, 1987) and extracted at $80 \mu\text{m}$ resolution through a centreline of the

1 FLS113 sediment core. MS was measured on the surface of the split sediment cores at 2 mm sample intervals with a Bartington
 2 MS2E point sensor using the CoreSusc MkIII core scanner.

3 The area between Vingersjøen and Flyginnsjøen (Fig. 4) is rich in glaciofluvial deposits easily remobilized whenever
 4 floods occur. Bifurcation events in Glomma causes precisely such a fundamental change in the erosion regime in this area,
 5 causing river-flooding in a normally dry area (see Sect. 3.2.1). The following calculations and interpretations are thus based
 6 on the assumption that bifurcations events can be recorded as marked increase in minerogenic input to lake Flyginnsjøen,
 7 redeposited from the pre-existing glaciofluvial deposits in the catchment.

8 To quantify the frequency of such events a local peak detection algorithm was applied on parameters sensitive to
 9 changes in minerogenic input. Flood deposits was defined as peaks in the measured parameters where (i) the measured
 10 concentration is higher than the two surrounding values, (ii) the difference between the peak and the lowest value within a
 11 specified time window (w) exceeds a specified threshold h_1 and, (iii) the difference between ~~the peak and the lowest value at~~
 12 ~~each sides of the peak (within the time window) exceeds a specified threshold h_2 where $h_2 < h_1$. Each~~The time lag between
 13 succeeding peak should be ~~separated~~ by at least 9 months. We chose a minimum -9-month time lag between two flood
 14 eventswindow since this catchment has one major flood event per year, mostly typically occurring in May/June. For locations
 15 with more frequent floods, a smaller time windowlag could be more appropriate.

16 To produce a Holocene flood record based on the sediment cores from Flyginnsjøen depth in core was transformed
 17 to time using Bacon age-depth modelling software (Blaauw and Christeny, 2011) (see Sect. 4.1.1), and frequency of events in
 18 50-year moving window was quantified. In order test to what extent the lake sediment records reproduce modern and historical
 19 observations, identified flood layers was compared to with instrumental streamflow data.

20

21 3.4 Flood frequency modelling

22 3.4.1 Stationary flood frequency modelling

23 A Generalized Extreme Value (GEV) distribution was invoked to establish a flood frequency model for floods at Elverum.
 24 The GEV distribution is shown to be a limiting distribution for block maxima (Embrechts et al., 1997; Fisher and Tippett,
 25 1928; Gnedenko, 1943):

26

$$27 F(x) = \begin{cases} \exp\left\{-\left[1 - k\left(\frac{x-m}{\alpha}\right)\right]^{1/k}\right\} & \text{if } k \neq 0 \\ \exp\left\{-\exp\left(-\frac{x-m}{\alpha}\right)\right\} & \text{if } k = 0 \text{ (Gumbel distribution)} \end{cases} \quad (1)$$

28

29 Where m is a location parameter, α a scale parameter and k a shape parameter. We estimated the parameters using a Bayesian
 30 approach. Their posterior density π^* ~~was~~ calculated as

31

$$32 \pi^*(m, \alpha, k | \vec{x}) = \frac{l(\vec{x} | m, \alpha, k) \pi(m, \alpha, k)}{\iiint l(\vec{x} | m, \alpha, k) \pi(m, \alpha, k) dm d\alpha dk} \quad (2)$$

33

34 Where π is the prior and $l(\vec{x} | m, \alpha, k)$ is the likelihood of the observation vector \vec{x} given the parameters m, α, k . The
 35 denominator makes the integral under the pdf equal one.

36 We used non-informative priors for the location and scale parameters, (i.e. the location parameter and the log-
 37 transformed scale parameter were uniform). A normal distribution with standard deviation 0.2 and expectation 0.0 was used
 38 as prior for the shape parameter k , inspired by Coles and Dixon (1999), Martins and Stedinger (2000), and Renard et al. (2013)

39 .

1 The likelihood for the systematic data is- (see Gaál et al., 2010; Stedinger and Cohn, 1986):

$$2$$
$$3 \quad l_s = \prod_{i=1}^n f(x_i|m, \alpha, k) \quad (3)$$

4 Where $f(x_i)$ is the probability density function for the GEV distribution with the parameter values m, α, k evaluated for the
5 observation x_i . For historical- and paleofloods, it is assumed that all g_j floods ~~that must~~ exceed a threshold $x_{0,j}$ for the period j
6 where duration h_j ~~are is~~ known. The likelihood of h_j - g_j number of floods not exceeding $x_{0,j}$ during the period h_j is given as:

$$7$$
$$8 \quad l_{b,j} = [F(x_{0,j}|m, \alpha, k)]^{h_j - g_j} \quad (4)$$

9

10 Where F is the GEV distribution given in Eq. (1).

11

12 We also need to include available knowledge on floods exceeding $x_{0,j}$. In the simplest case we know only that g_j floods exceeded
13 $x_{0,j}$, if so likelihood can be written as:

$$14$$
$$15 \quad l_{a1,j} = [1 - F(x_0|m, \alpha, k)]^{g_j} \quad (5)$$

16

17 Alternatively, we might know that the floods that exceeded x_0 took place within an interval defined by an upper x_U and lower
18 x_L limit:

$$19$$
$$20 \quad l_{a2,j} = \prod_{o=1}^{g_j} [F(x_{U,o}|m, \alpha, k) - F(x_{L,o}|m, \alpha, k)] \quad (6)$$

21

22 And, in optimal scenario, we know the exact magnitude of all floods exceeding $x_{0,j}$:

$$23 \quad l_{a3,j} = \prod_{o=1}^{g_j} f(y_o|m, \alpha, k) \quad (7)$$

24

25 The total likelihood is given as a product of the three major likelihood terms:

$$26 \quad l_i = l_s \prod_{j=1}^J l_{ai,j} l_{b,j} \quad (8)$$

27

28 Where J is the number of sub-periods with specific perception thresholds.

29 The posterior distribution of the parameters was estimated using a MCMC-method implemented in the R-package
30 nsRFA (Vigliano, 2012). For estimating return levels, we used the posterior modal values of the parameters. It poses a
31 challenge to set the perception threshold x_0 and length of the historical floods h , i.e. for which period the listed floods represents
32 all floods above the threshold. A simple rule is to set the perception threshold to the lowest observed historical flood value in
33 the historical period. The length of the historical period was decided using the average spacing approach as recommended by
34 Engeland et al. (2018) and Prosdocimi (2018).

35

36 3.4.2 Plotting position

37 The plotting positions from provided by Hirsch and Stedinger (1987) that is based builds on the Cunnane plotting position
38 (Cunnane 1978) were used to plot the empirical distribution of the observations. The exceedance probability p_i of x_i with rank
39 i from a data set with t historical floods representing the historic period h , and s systematic floods with e extraordinary floods
40 is given as:

$$p_i = \frac{i-0.4}{l+0.2} \cdot \frac{l}{n} \quad i = 1, \dots, l$$

$$p_i = \frac{l}{n} + \frac{n-l}{n} \cdot \frac{i-l-0.4}{s-e+0.2} \quad i = l+1, \dots, t+s \quad (9)$$

where i is the rank, l is the number of extraordinary floods ($l = t + e$) and n is the length of the period for which we have information about floods (note that $n = h + s$)

3.4.2 Non-stationary flood frequency modelling

We applied a simple approach to get an estimate of the non-stationary 200-year flood during the recent 1000 year using the paleorecord. In a first step the parameters m' , α' and k' in the GEV distribution were estimated using the systematic flood observations. Then we ~~can~~ estimated the flood quantiles as:

$$x(F|m', \alpha', k') = \begin{cases} m' + \frac{\alpha'}{k'} [1 - (1 - \ln(F))^{k'}] & k' \neq 0 \\ m' - \alpha' [\ln(-\ln(F))] & k' = 0 \end{cases} \quad (109)$$

Note that by replacing F with $1-1/T$ in Eq. (109) we ~~could~~ calculate the flood quantiles for the return period T .

From the sediment core we ~~can~~ estimated a time series of the probability of exceedance w_t of the threshold u , for each year t ~~by if we calculate~~ the exceedance rates w_t as the mean number of excesses in a sufficiently large moving window. ~~If Further,~~ we assumed ed that the observed non-stationary exceedance rate influenced s both the location and scale parameters with a common factor r_t . ~~we see f~~ From Eq. (109) we found that

$$x(F = 1 - w_t | r_t m', r_t \alpha', k') = r_t x(F = 1 - w_t | m', \alpha', k') = v \quad (110)$$

Since the threshold v , and the exceedance rate w_t is known, the factor r_t can be estimated as:

$$r_t = v / x(F = 1 - w_t | m', \alpha', k') \quad (12+)$$

The T -years flood for the time t can then be estimated as:

$$q_{Tt} = r_t x(F = 1 - 1/T | m', \alpha', k') \quad (132)$$

4 Results

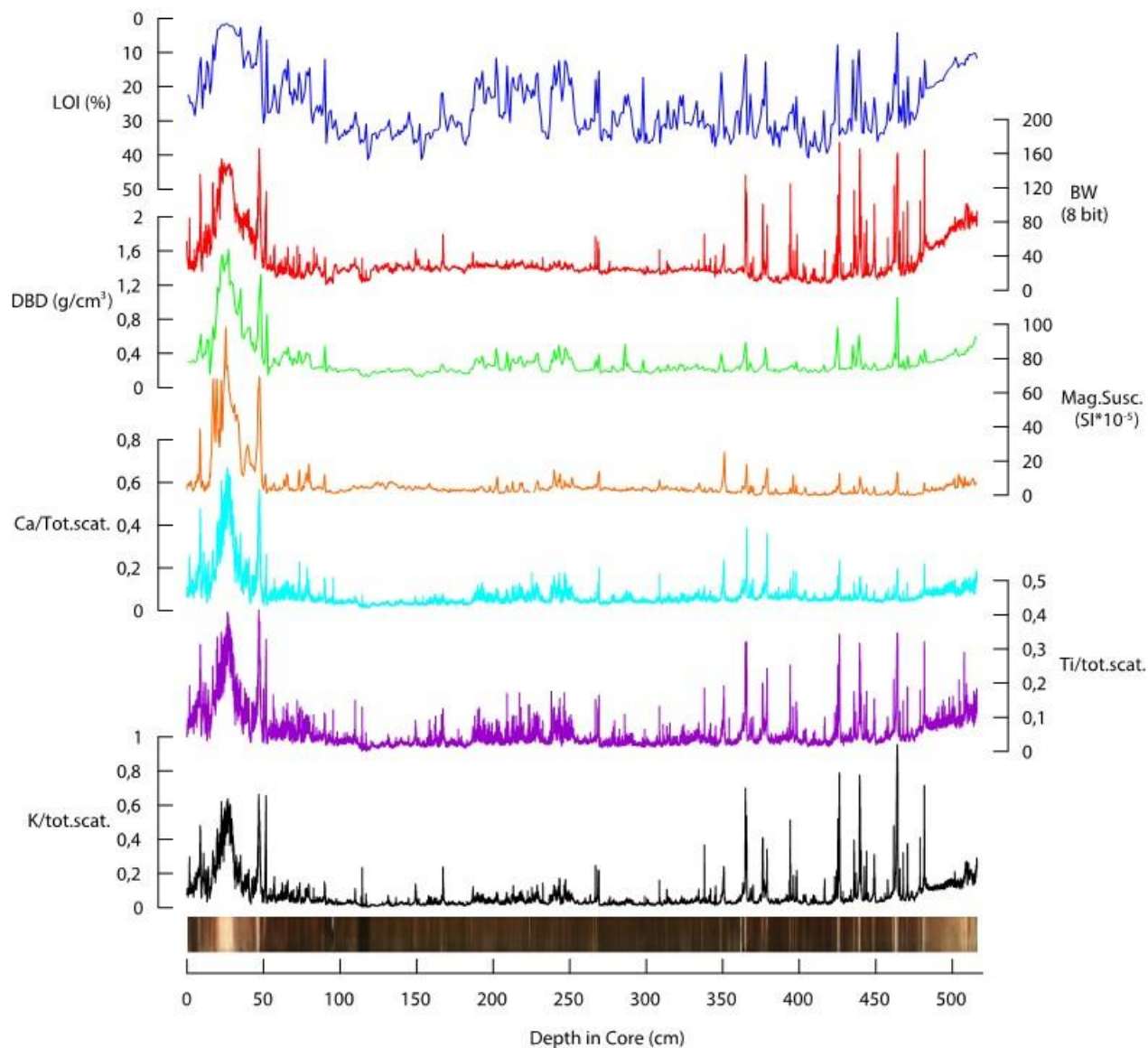
4.1 Flood variability from the lake sediment cores

The shortest core (FLS113) is 18 cm long, and represent the period ~~AD~~ 1953-2013 (se Fig. 11). The longest core (FLP213) is 516 cm long and represents the period approximately 0-10 300 years before present (present = 1950) (see Table 5 and Fig. 11).

FLP213

The results from the XRF-scan ($Ti_{total\ scatter}$, $Ca_{total\ scatter}$ and $K_{total\ scatter}$) and the greyscale-value (BW) from photo of the core are shown as a function of depth in Fig. 9 together with a photo of FLP213. The core consists of a dark brown gyttja with preserved macro fossils including leaf fragments. This gyttja, carrying a low minerogenic content, is referred to here as 'the background signal' which is characterized by its dark color (BW<30), high LOI (30-40%), low DBD (<0.3 g/cm³) and magnetic susceptibility (MS) with values close to zero (<5 SI*10⁻⁵). Moreover, it returns low $K_{total\ scatter}$ (<0.03), $Ti_{total\ scatter}$ (<0.03) and $Ca_{total\ scatter}$ (<0.03). Interspersed in this 'organic slush' there are narrow (mm scale) light grey (BW 40-170) minerogenic layers with LOI lower than 20%, relatively high density (DBD 0.5-1.0 g/cm³), higher than average MS with peaks at 15-20 SI*10⁻⁵ as well as peaks in $K_{total\ scatter}$ (0.1-0.9), $Ti_{total\ scatter}$ (0.1-0.4) and $Ca_{total\ scatter}$ (0.1-0.7). At 33.5-18.0 cm depth in core there is an anomalous thick minerogenic layer with LOI at <2%, DBD at 1.6 (g/cm³), MS at 98 SI*10⁻⁵, and very high $K_{total\ scatter}$ (0.6), $Ti_{total\ scatter}$ (0.4) and $Ca_{total\ scatter}$ (0.7).

1 The correlation matrix (Table 3) shows strong (and significant) correlations between $K_{total\ scatter}$, $Ti_{total\ scatter}$, Ca_{total}
 2 $scatter$, MS and BW. The weakest correlation is 0.74 between MS and BW which is still very high. LOI is, as expected, negatively
 3 correlated with all the other measured variables. We suggest that the main process explaining the relationships between these
 4 parameters is driven by the on-off signal related to transport of minerogenic material to Flyginnsjøen during bifurcation events.
 5
 6



7
 8 Figure 9: Results from measured parameters in FLP213. Loss-on-ignition (LOI %) indicated content of organic matter in the
 9 core, and are plotted on an inverse scale (blue). BW (red) shows the 8-bit (0-255) black-white values extracted from a photo
 10 of the core surface where 0 is black. Dry bulk density (DBD) is plotted in unit gram per cm³ (green). Magnetic susceptibility
 11 (orange) is plotted as SI*10⁻⁵ as magnetic susceptibility is a dimensionless parameter. XRF-data (K, Ca and Ti) are normalized
 12 against total scatter to reduce potential effect of water content.

13
 14
 15
 16
 17
 18

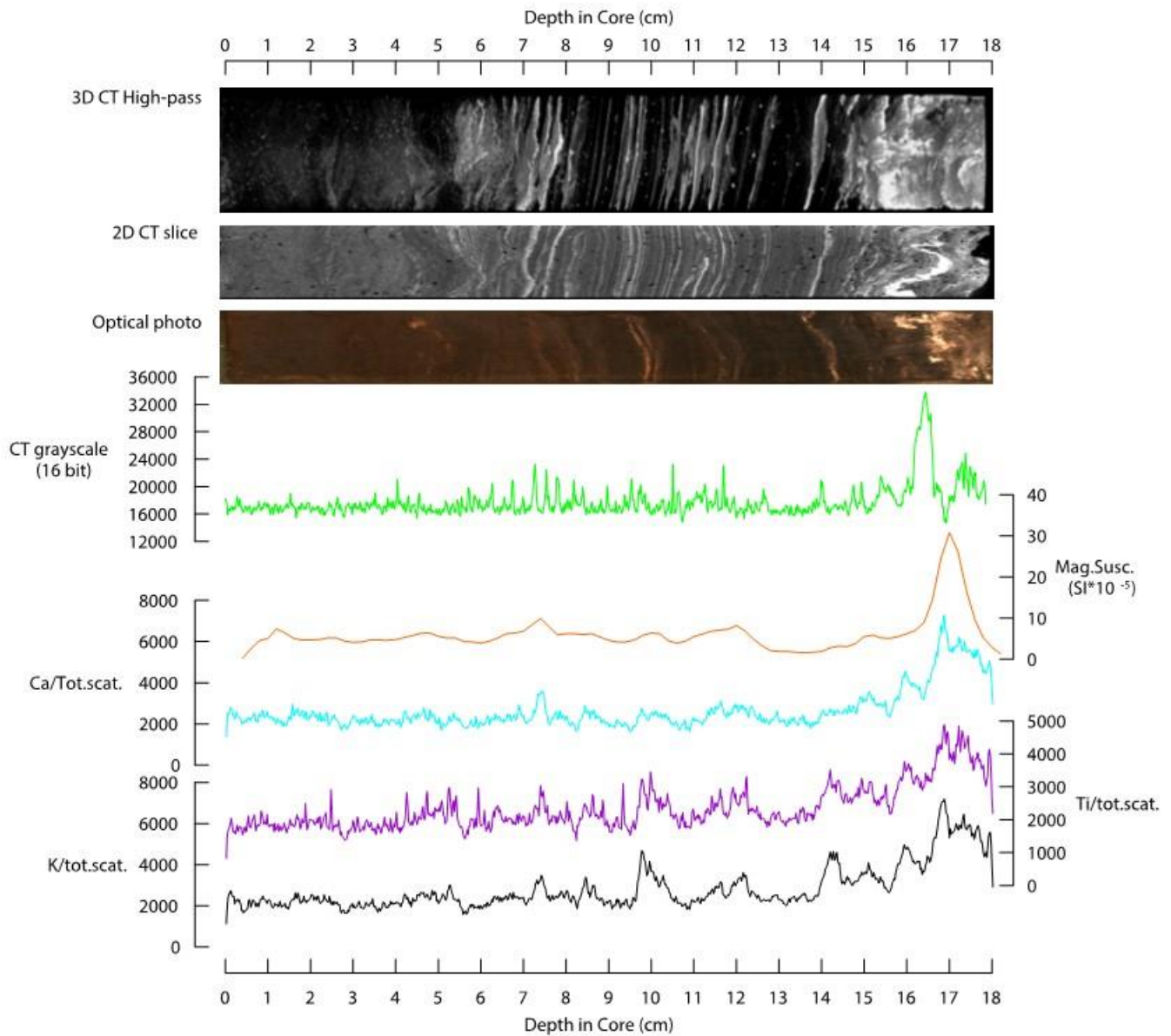
Table 3 Correlation between measured parameters in FLP213 (*in bold*) and FLS113 (*in italic*). LoI, BW, DBD, MS and the XRF-data (K, Ca and Ti) were measured in FLP213 whereas CT greyscale, MS and the XRF-data (K, Ca and Ti) were measured in FLP113. LOI (-%) indicate content of organic matter in the core, BW is the 8-bit (0-255) black-white values extracted from a photo of the core surface where 0 is black. CT greyscale is a 16-bit number indicate relative densities of the core, DBD is given in unit gram per cm³ (green). MS is measured as SI*10⁻⁵ (it is a dimensionless parameter). XRF-data (K, Ca and Ti) are normalized against total scatter to reduce effect of water content. All correlations are significantly different from zero.

	LoI	BW	CT greyscale	DBD	MS	K _{/total scatter}	Ca _{/total scatter}	Ti _{/total scatter}
LoI	1	-0.67 / -	- / -	-0.82 / -	-0.61 / -	-0.61 / -	-0.64 / -	-0.67 / -
BW	-0.67 / -	1	- / -	0.82 / -	0.74 / <i>-0.73</i>	0.89 / -	0.81 / -	0.89 / -
CT greyscale	<i>- / -</i>	<i>- / -</i>	1	- / -	<i>- / 0.79</i>	<i>- / 0.64</i>	<i>- / 0.68</i>	<i>- / 0.59</i>
DBD	-0.82 / -	0.82 / -	- / -	1	0.86 / -	0.77 / -	0.87 / -	0.82 / -
MS	-0.61 / -	0.74 / <i>-0.73</i>	<i>- / 0.79</i>	0.86 / -	1	0.76 / <i>0.66</i>	0.86 / <i>0.73</i>	0.76 / <i>0.63</i>
K _{/total scatter}	-0.61 / -	0.89 / -	<i>- / 0.64</i>	0.77 / -	0.76 / <i>0.66</i>	1	0.85 / <i>0.93</i>	0.96 / <i>0.95</i>
Ca _{/total scatter}	-0.64 / -	0.81 / -	<i>- / 0.68</i>	0.87 / -	0.86 / <i>0.73</i>	0.85 / <i>0.93</i>	1	0.91 / <i>0.88</i>
Ti _{/total scatter}	-0.67 / -	0.89 / -	<i>- / 0.59</i>	0.82 / -	0.76 / <i>0.63</i>	0.96 / <i>0.95</i>	0.91 / <i>0.88</i>	1

FLS113

This core shows dark organic gyttja with light grey minerogenic layers, similarly to FLS213. The minerogenic layers yield high values of K_{/total scatter} (0.2-0.8), Ca_{/total scatter} (0.1-0.4) and Ti_{/total scatter} (0.1-0.2) as well as slight increase in MS (>6 SI*10⁻⁵) (Fig. 10). CT data shows that the light grey layers are of high density and reveals numerous thinner layers not visible on photo or in the lower-resolution XRF and MS data. Slight offsets in the positioning of layers in the CT imagery and optical photo occurs due to the fact that the layering is not entirely horizontal.

Correlation coefficients between CT greyscale values, MS, K_{/total scatter}, Ca_{/total scatter} and Ti_{/total scatter} in FLS 113 are all over 0.59 and significantly larger than zero. The strongest correlation is seen between K_{/total scatter}, Ca_{/total scatter} and Ti_{/total scatter} (Table 3). The somewhat weaker correlation to MS and CT greyscale, and the fact that CT imagery show layering (e.g. 11-12 cm depth in core) not picked up by the other data (Fig. 10), can partly be explained by slight offsets in the positioning of layers between the different scans as well as differences in sampling resolution. The strong correlations and general picture of layered intervals yielding high values, however, indicates that one dominating factor ‘controls’ the variability, providing further support of the interpretation that transport of minerogenic material to Flyginnsjøen during bifurcation events is the main process.



1
 2 Figure 10: Results from high resolution analysis of core FLS113. The top panel shows a 3D CT-visualization of high-density
 3 layers (white) in the core. The 2D slice is an 80 μ m thick slice from the middle of the sediment core. The Optical photo is an
 4 RGB photo of the surface of the halved sediment core. CT grayscale plot (green) shows an 80 μ m grayscale variability along
 5 a line through the middle of the sediment core. MS (orange) is plotted as $SI \cdot 10^{-5}$ as magnetic susceptibility is a dimensionless
 6 parameter. XRF-data (K, Ca and Ti) are normalized against total scatter to reduce effect of water content.

8 4.1.1 Age-depth models

9 To establish an age-depth relationship for the cores, sediments were subjected to lead dating ^{210}Pb (FLS113) and radiocarbon
 10 dating (^{14}C) of FLP213. Measurements were performed by the Environmental Radioactive Research Center at the University
 11 of Liverpool (Appleby and Piliposian, 2014) and Poland (Poznan Radiocarbon Laboratory) (Goslar, 2014). The ^{210}Pb and ^{14}C
 12 dates used to establish the age-depth models presented in Fig. 11 are listed in Table 4 and 5. Estimation of age as a function
 13 of depth for FLS113 was done using a quadratic term regression model of CRS model calculations of the ^{210}Pb with the 1963
 14 ^{137}Cs peak at 16.25 cm depth in core (Table 4) as a reference point (Appleby, 2001). For FLP213, we used a Bacon age-depth
 15 modelling approach (Blaauw and Christeny, 2011) available in the R-package Bacon. One ^{14}C sample from 51 cm depth in
 16 FLP213 was rejected, as this has a stratigraphically reversed age (see Table 5). The age is clearly too old, possibly related to

1 high content of saw dust bringing in relative old carbon core at depth in core. The saw dust may have originated from a saw
 2 mill in the catchment at this time. The 15.5 cm thick anomalous layer at 18.0-33.5 cm depth in core was classified as “slump”
 3 in the Bacon model, and thus interpreted as an instantaneous event deposit. This layer has a basal age estimate of 1776 CE
 4 from the age-model, and is likely to be related to the historically documented 1789 CE Stor-Ofsen flood event (see Sect. 3.2).
 5

6 Table 4: Fallout radionuclide concentrations and chronology for FLS113 from Flyginnsjøen.

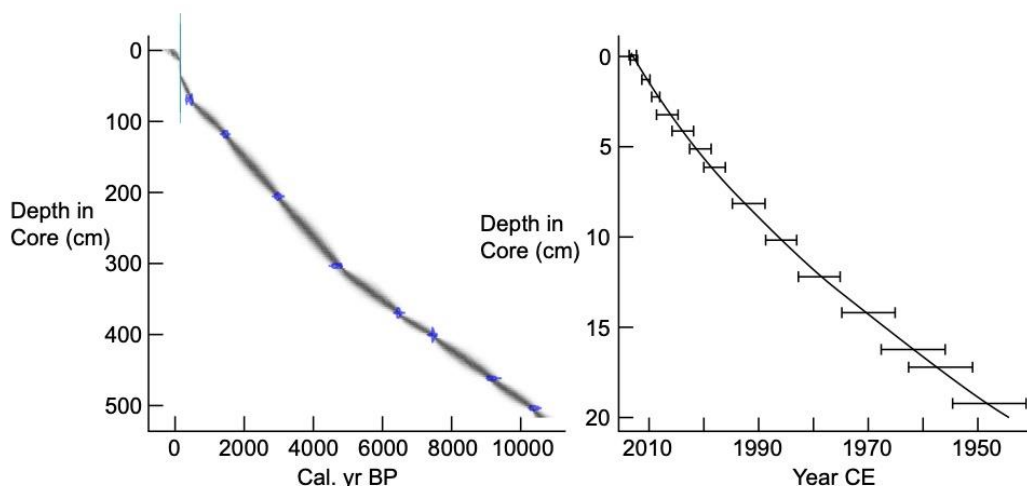
Depth (cm)	$^{210}\text{Pb}_{\text{Total}}$ (Bq kg $^{-1}$)	\pm	$^{210}\text{Pb}_{\text{Unsupp.}}$ (Bq kg $^{-1}$)	\pm	$^{210}\text{Pb}_{\text{Supp.}}$ (Bq kg $^{-1}$)	\pm	^{137}Cs (Bq kg $^{-1}$)	\pm	Year	Uncertainty (years)
0									2013	1
0.25	809.5	47.9	702.3	49.2	107.2	11.3	65.7	7.2	2013	1
1.25	686.2	33.4	585.9	34.0	100.3	6.6	63.3	5.3	2011	1
2.25	570.9	21.6	492.4	21.9	78.5	3.9	62.0	3.4	2009	1
3.25	598.8	22.6	524.3	23.0	74.5	4.2	72.7	3.7	2007	2
4.25	549.2	21.5	474.9	21.9	74.2	3.9	82.9	4.3	2004	2
5.25	455.9	17.5	386.0	17.8	69.8	3.1	77.6	3.4	2000	2
6.25	482.0	25.2	404.0	25.6	78.0	4.7	64.0	3.9	1998	2
8.25	515.6	20.4	442.3	20.7	73.2	3.7	58.9	3.3	1992	3
10.25	391.4	19.3	329.6	19.6	61.8	3.6	84.6	3.7	1986	3
12.25	331.6	15.3	266.2	15.6	65.4	3.0	78.1	3.1	1979	4
14.25	231.2	12.8	173.4	13.1	57.9	2.6	68.0	2.8	1970	5
16.25	226.4	13.8	152.8	14.1	73.7	3.1	138.8	4.1	1962	6
17.25	193.3	13.3	140.7	13.5	52.6	2.7	50.7	2.4	1957	6
19.25	112.9	7.3	68.8	7.4	44.1	1.6	9.2	1.2	1948	7

7

8 Table 5: ^{14}C -dates for FLP213 from Flyginnsjøen. Radiocarbon ages are calibrated using the IntCal 13 calibration curve
 9 (Reimer et al., 2013)

Lab. Nr.	Depth in core (cm)	^{14}C age, yr BP	Cal. yr BP (most prob. 68.3% conf int.)
Poz-57974	51	870 \pm 30	732 – 796 (0.97)
Poz-59030	70	390 \pm 30	453 – 503 (0.78)
Poz-57975	118	1565 \pm 35	1455 – 1521 (0.73)
Poz-57976	206	2860 \pm 40	2924 – 3037 (0.91)
Poz-57977	304	4125 \pm 40	4571 – 4653 (0.49)
Poz-57978	370	5670 \pm 40	6409 – 6487 (1.00)
Poz-59029	401	6535 \pm 35	7424 – 7476 (1.00)
Poz-57979	462	8180 \pm 50	9028 – 9140 (0.75)
Poz-57980	504	9190 \pm 50	10259 – 10403 (1.00)

10



11

12 Figure 11 Age-depth model for FLP213 (right) and FLS113 (left). Note the step in the FLP213 age-depth model at 33.5 – 18.0
 13 cm depth in core related to the *Stor-Ofsen* flood event in 1789 CE.

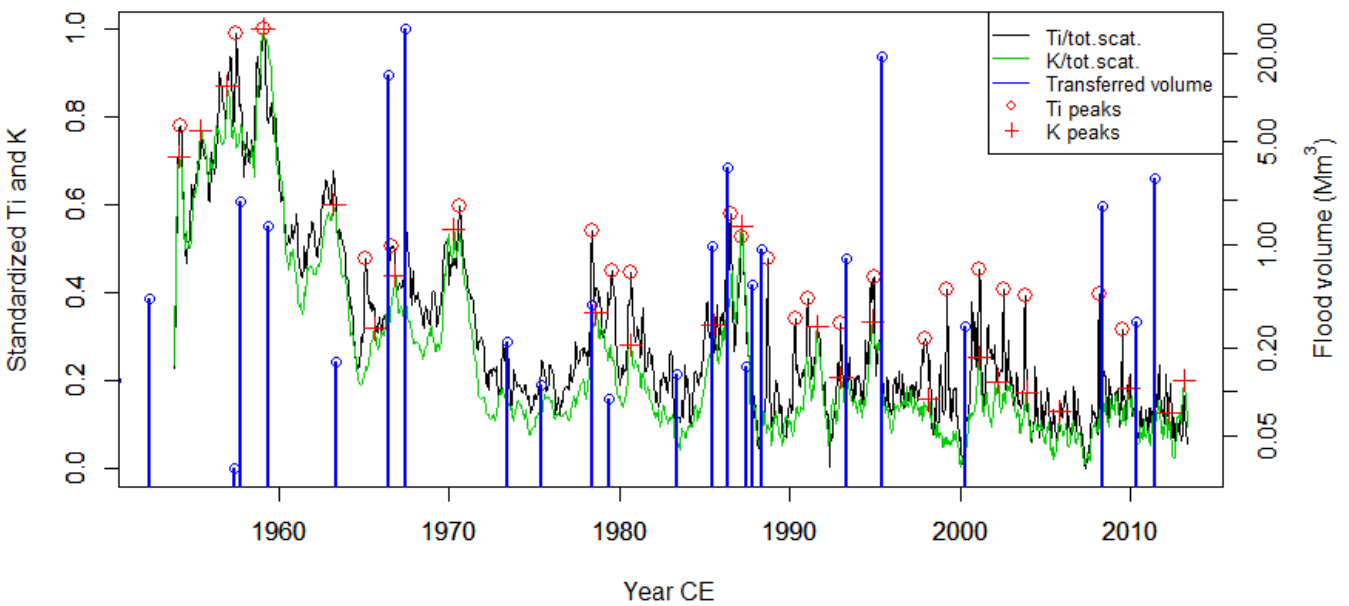
1

2 4.1.3 Identification of flood layers in FLS113.

3 We used the concentration of $Ti_{total\ scatter}$ and $K_{total\ scatter}$ from the XRF-scan of FLS113 to establish a link between dense,
 4 minerogenic sediment layers and the 22 bifurcation events between 1953 and 2013. Note that XRF data ($K_{total\ scatter}$, $Ca_{total\ scatter}$
 5 and $Ti_{total\ scatter}$) correlates strongly with the CT-scan (greyscale values), and MS for both FLS113 and FLP213 (Table 3), and
 6 this suggests the flood transported material originate from a one source and that this is constant over time. All detected layers
 7 are thus interpreted to be related to the same process bringing minerogenic material to Flyginnsjøen. The first step in our
 8 approach was to transform the depth of the XRF-scan to age using the depth-age model for FLS113. After having identified
 9 the flood layers, we used the algorithm described in Sect. 3.3.1 to identify local peaks in the measured parameter. We used a
 10 time window of 1 year, a value of 680 and 527 for $Ti_{total\ scatter}$ and $K_{total\ scatter}$ respectively for h_1 and $h_2=0.5 * h_1$ which identified
 11 23 local peaks for $Ti_{total\ scatter}$ and $K_{total\ scatter}$ over the same period that we observe 22 bifurcation events. A time series of the
 12 bifurcation volumes and the XRF-scan data can be viewed in Fig. 12. Taking into account the uncertainty in the dating (Fig.
 13 11), we see that five of the bifurcation events do not correspond directly to a sediment layer. All the three largest flood events
 14 were, however, correctly identified, and considering the uncertainties in the age-depth model this supports our working
 15 hypothesis that sediment layers can be used to identify flood events caused by episodes of bifurcation at Kongsvinger.

16

17



18

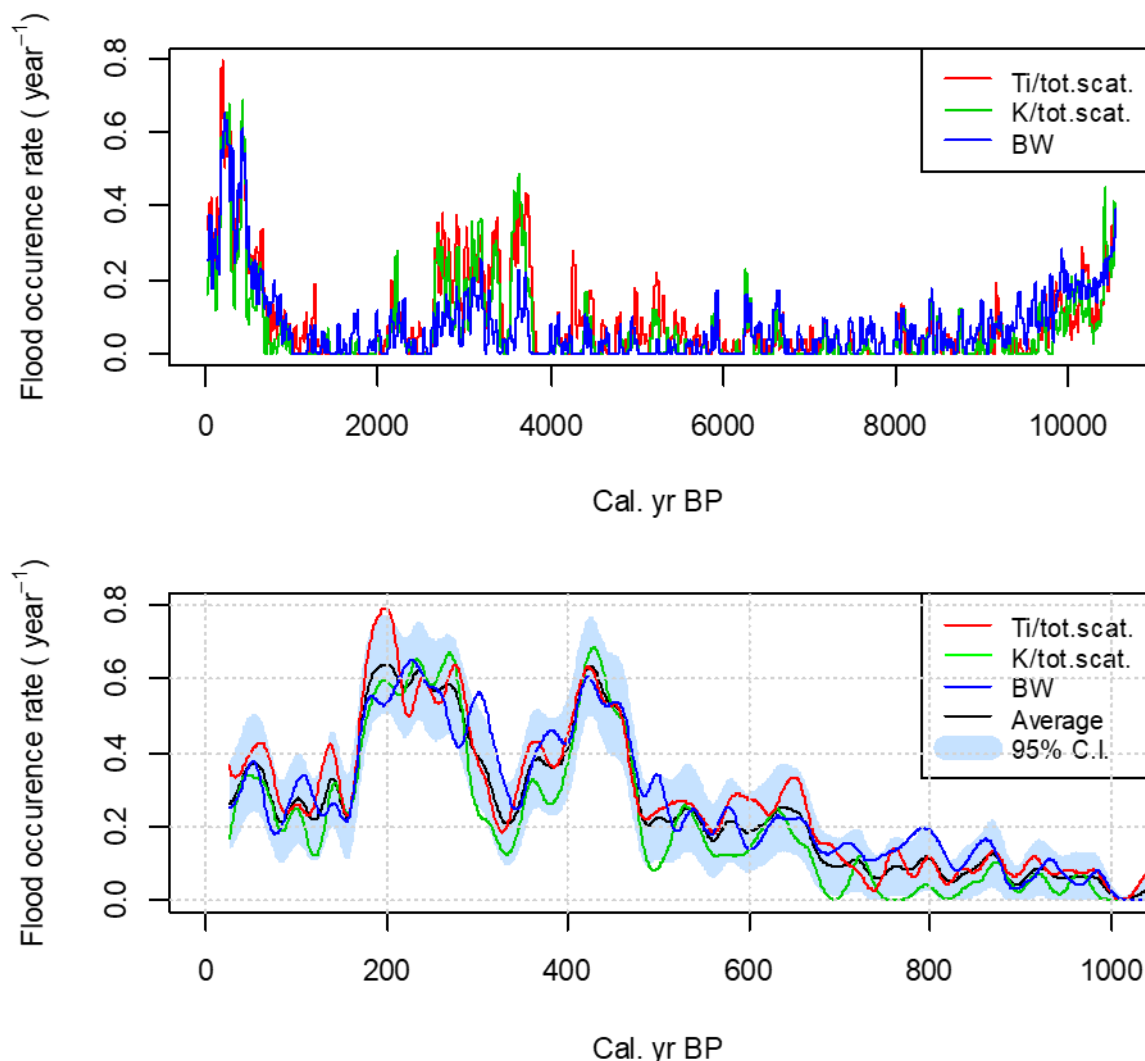
19 Figure 12. Transferred volume of the 23 bifurcation events in the period 1950-2013 CE (in blue) and the 24 identified flood-
 20 layers (red) identified using XRF scans of $Ti_{total\ scatter}$ and $K_{total\ scatter}$ for FLS113.

21

22 4.1.3 Frequency of flood events during the Holocene.

23 From FLS113 we have established a link between dense, minerogenic sediment layers and bifurcation events. We therefore
 24 assumed that the analyses of FLP213 ~~couldan~~ be used to produce a time series of flood events covering the last 10 300 years.
 25 Here we ~~have~~ used the local peak detection algorithm presented above to identify sediment layers with high concentration of
 26 $K_{total\ scatter}$ and $Ti_{total\ scatter}$. Since the uncertainty range in the age estimate is 30 to 50 years, we calculate the average rate of a
 27 given flood event within a moving Gaussian time windows of 50 years for both $Ti_{total\ scatter}$ and $K_{total\ scatter}$ (Fig. 13). The standard

1 deviation of the estimated flood rate $\hat{\lambda}$ was calculated as $\hat{\lambda} \pm z \sqrt{\frac{\hat{\lambda}(1-\hat{\lambda})}{50}}$ and it was used to assess the 95% confidence intervals.
 2 We see that the flood counts using $Ti_{total\ scatter}$, $K_{total\ scatter}$ and BW to a large degree overlap and follow the same Holocene
 3 trends, as anticipated due to the high correlation coefficient between the two (see above).



4
 5 Figure 13: In the top panel, average flood rate per year calculated in a 50-years moving window during the Holocene. In the
 6 lower panel, the recent 1000 years are shown only. The lower panel also include a 95% confidence interval for the average
 7 flood rates. The flood rates were identified by detecting local peaks in $Ti_{total\ scatter}$, $K_{total\ scatter}$ and BW values.
 8

9 4.2 Stationarity of flood frequency in the paleo-flood data

10 A key observation in the Holocene flood frequency reconstruction is the large non-stationarity played out across multiple time
 11 scales. We observe that there are two major flood rich periods during the Holocene (Fig. 13, upper panel). The first runs from
 12 3800 to 2000 cal. yr BP when it ends abruptly. The second period extend from around 7600 cal. yr BP up to present day.
 13 Looking at flood frequency over the recent 1000 years (Fig. 13, lower panel) we observe significant internal variability within
 14 the flood rich period. The period with the highest flood rates occurs in the 18th century, but also in the 15th century. ~~The high
 15 flood frequency in the 18th century is also recorded in the historical flood data (Fig. 6).~~ The data from FLP213 informs us that
 16 the flood event in 1789 is truly an anomaly, as is evident from the sheer amount of sediments deposited during this event (no
 17 other flood comes close), and it also yield the highest measured values of e.g. density (DBD) as well as magnetic susceptibility

1 (MS) throughout the core (Fig. 9). It is therefore reasonable to assume that the 1789 CE flood was an extraordinary event
 2 making it the largest during the entire time span of the record, i.e. 10 300 years.

3

4 4.3 Flood quantile estimation by combining systematic-, historical- and paleo-flood data

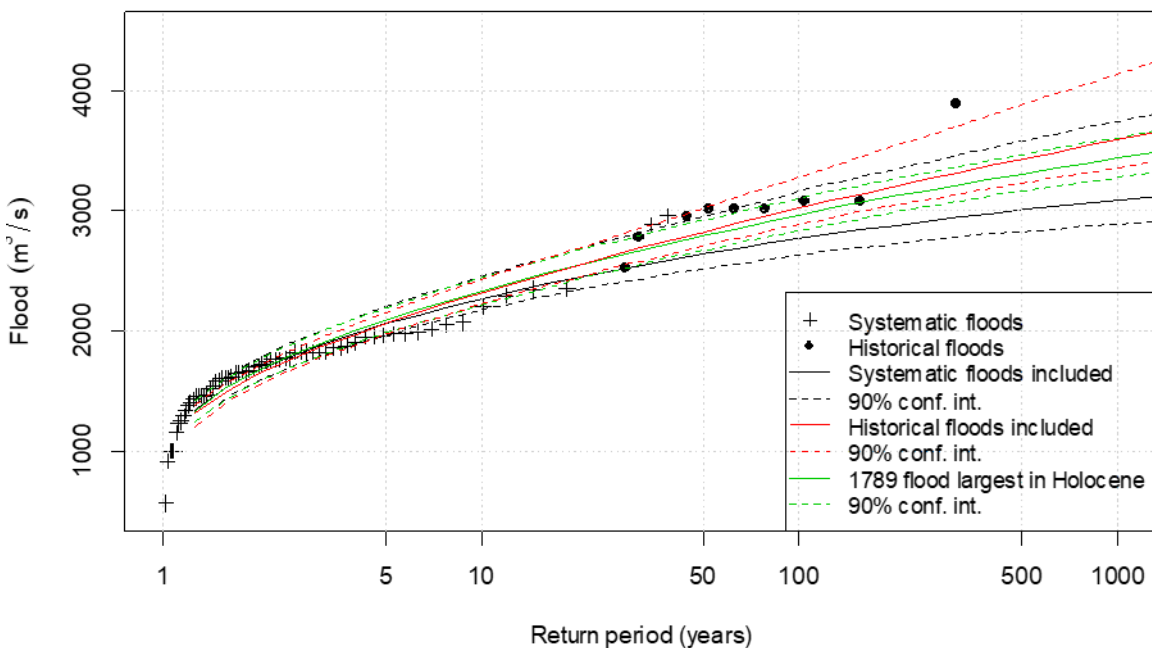
5 The flood quantiles combining the systematic, historical and paleodata have been analysed in different, but complementary
 6 ways. Table 6 provides an overview over of the flood information in each related to data source and the time spans intervals they
 7 represent. The first step in this approach was to estimate the flood quantiles using only systematic data. In the second approach
 8 whereupon we added included all the historical flood data. The smallest historical flood of 2533 m³/s was used as the threshold
 9 x₀. The length of the historical data period was calculated based on Prosdocimi (2018) and Engeland et al. (2018). The smallest
 10 historical flood of 2533 m³/s was used as the threshold x₀. Since t The average waiting time between the historical floods is 22
 11 years, the start of for the historical period was set to be 22 years before CE 1675 (i.e. the year of the oldest historical flood) that
 12 started in 1653 CE and The historical period ended in CE 1871 giving $h = 219$ years. The exact sizes of the historical
 13 floods (Table 1) was assumed. In the third approach we used the paleo-record as a guidance to weigh the historical information.
 14 Since paleorecord indicates that the historical floods in the 18th century occurred in a flood rich period, we used only the
 15 historical flood events from the 19th century. Moreover, the historical flood from CE 1789 was included, and it was
 16 suggested that this was the largest flood during the last 10 000 years for reasons explained above. The results are shown in
 17 Fig. 14, and we see that the results are sensitive to the assumption of which period the CE 1789 flood represents.

18

19 Table 6 Overview over the three data sources used for flood frequency analysis.

<u>Data source</u>	<u>Period</u>	<u># floods</u>	<u>Threshold (m³/s)</u>
<u>Systematic flood data</u>	<u>1872-1936</u>	<u>=</u>	<u>=</u>
<u>Historical flood data</u>	<u>1653-1871</u>	<u>9</u>	<u>2533</u>
<u>Paleo Flood data</u>	<u>1300-1871</u>	<u>208</u>	<u>1800</u>
<u>Paleo Flood data when combined with historical flood data</u>	<u>1300-1651</u>	<u>110</u>	<u>1800</u>

20



21

Figure 14: The sensitivity of flood frequency analysis to three different combinations of systematic and historical flood data. Annual maximum floods for the period 1872-1836 were used as systematic flood data.- Nine historical floods exceeding 2533 m³/s and representing the period 1653-1871 were used as historical floods. Based on the paleorecord, the CE 1789 flood was reweighted to represent a period of 10 000 years. The plotting positions for the systematic and historical floods are based on Hirsch and Stedinger (1987) and explained in Section 3.4.2.

The next step was to include the paleo-flood information in the flood frequency analysis. We did this in two ways: (i) we combined the systematic data and the paleodata and (ii) we combined systematic, historical and paleodata. For the paleodata we used 1800 m³/s as the threshold x_0 since it provided the same number of flood events (i.e. 19 events) from the paleo record and the streamflow observations for the overlapping time period (1891-1950). ~~In case (ii) above, When we combined the systematic data and the paleodata we counted 20894 flood events representing a period of 572330 years (13020-1871650 CE), and for case (iii), When we combined the systematic, historical and paleodata, we counted 11079 events for a period of 353540 years (13020-168520 CE) from the paleodata and used the 9 historical floods representing the period 1653-1871.~~ The results are shown in Fig. 15. We see that the estimates are sensitive to historical information. The paleodata did not impact the result to the same degree.

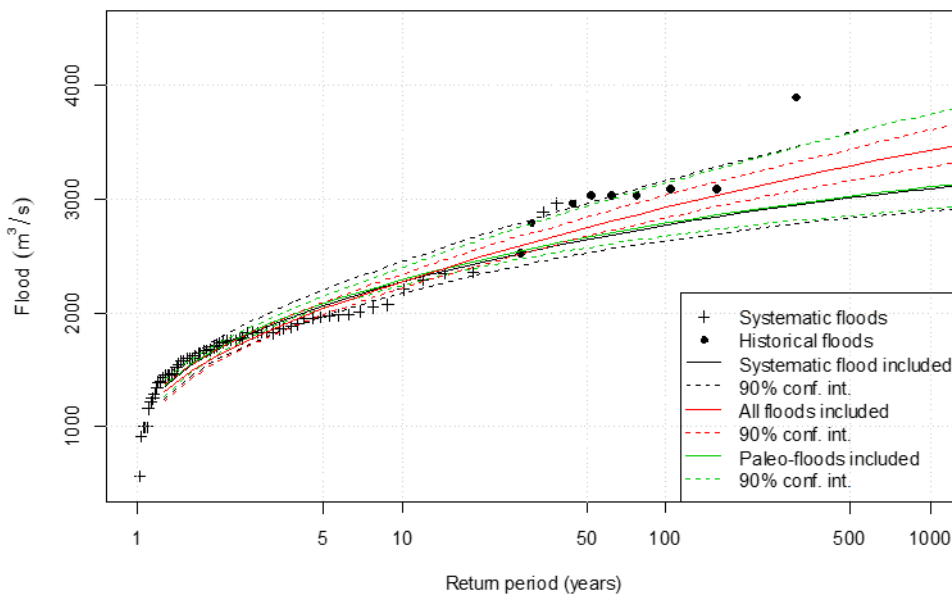
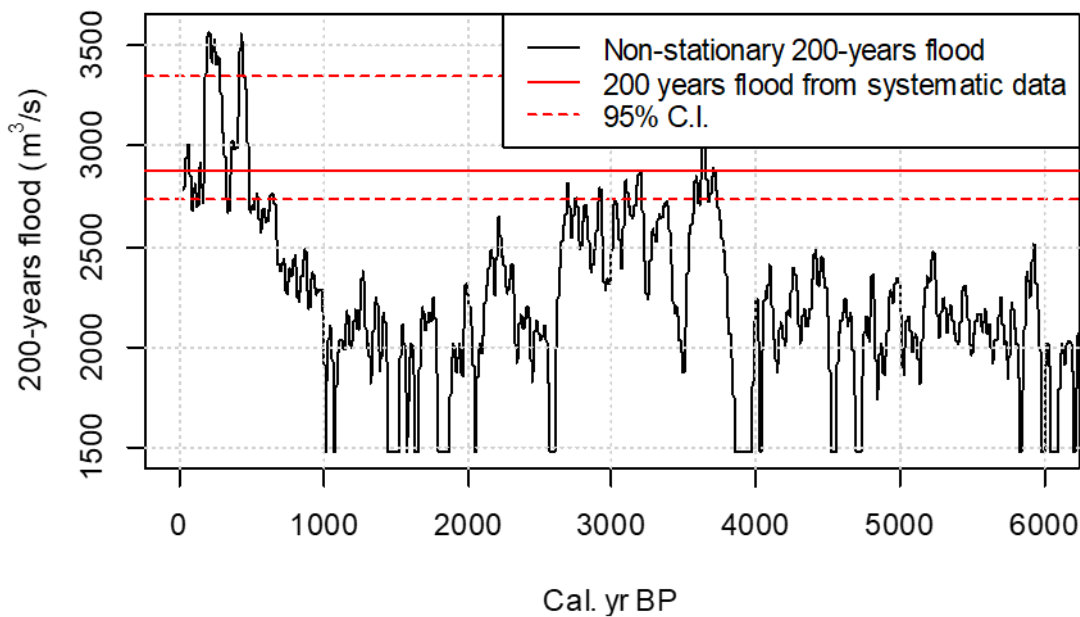


Figure 15. The sensitivity of flood frequency analysis to three different combinations of systematic, paleo, and historical flood data. Annual maximum floods for the period 1872-1836 were used as systematic flood data. Paleo-floods representing 208 events exceeding 1800 m³/s for the period 1300-1871. When all flood data were combined, the paleo-floods represent 110 events for the period 1300-1652, and -nine historical floods exceeding 2533 m³/s and representing the period 1653-1871 were used as historical floods. ~~using paleoflood data.~~ The plotting positions for the systematic and historical floods are based on Hirsch and Stedinger (1987) and explained in Section 3.4.2.

To achieve a nonstationary estimate of the design flood, we used the flood occurrence rate presented in Fig. 13 to estimate the 200-years flood in a moving time window as explained in Sect. 3.4.2. We used 1900 m³/s as the threshold v in Eq. (11) since it provided a good agreement between the 200-years flood estimated from the systematic data and the non-stationary 200-years flood for the overlapping period. The results are presented in Fig. 16. We now see that the size of the 200-years flood is non-stationary. During the ‘Little Ice Age’ (LIA) it was up to 23% higher than in present climate, whereas during the period 4000-6000 B.P it was around 30% lower than today.



1

2 Figure 16: Non-stationary estimate of the 200-years flood for the resent 6000 years. The red lines indicate the estimated 200-
 3 years flood and the 95% confidence intervals estimated using systematic streamflow observations.

4 5.0 Discussion

5 5.1 The reliability of the historical data and the paleoflood records

6 The historical data applied in this study are marked as water levels at the flood stone at Elverum, and the associated flood
 7 discharges are estimated by Hegge (1969). An assumption for these estimates areis that the river profile is relatively stable
 8 forover the historical period, and in particular that the large flood in CE 1789 did not cause make-any substantial changes. This
 9 is a reasonable assumption because, although since-four large floods occurred between CE 1781 – 1969, only one rating curve
 10 is used for the period-1781—1969, a period with four large floods. The gauging station was moved around 660 meters in 1969.

11 During the last decade or so lakes across Europe have been studied in detail and high-resolution paleoflood records
 12 have been produced from both the low-lands and the high-lands (see e.g.Cf. Wilhelm et al., 2018). Unlike many of these
 13 studies, we have worked with lakes that *only* receive flood-delivered sediments whenever the local river (Glomma) exceeds a
 14 certain well-known threshold (1500 m³/s). This setting tends to suggest that not only are we working with a sedimentary
 15 archive that filters out noise, but also one that provides a minimum estimate of the discharge associated with the floods
 16 recorded. The flood information extracted from the lake sediment cores, nevertheless, relies on a set of assumptions that is
 17 discussed in the following.

18 The first assumption is that all flood events recorded in lake Flyginnsjøen are directly related to Glomma. Linking the
 19 sedimentary signal in FLS113 to specific individual flood events in Fig. 12 is challenging. Due to the uncertainties in the age-
 20 depth model we have not found a good way to estimate probabilities for correspondence. Consequently, we rest on the
 21 assumption that our 23 recognized peaks in the sedimentary signal corresponds to the 24 bifurcation events over the same
 22 period based on the visual correspondence between peaks in K and Ti and flood volumes shown in Fig 12. We cannot
 23 completely rule out the possibility that minor floods in the local catchment of Flyginnsjøen occurred simultaneously with
 24 floods originating from Glomma or even just within the very small catchment surrounding the lake due to local rainstorm
 25 events. Given the heavy vegetation cover in the catchment of Flyginnsjøen, its small size and the low-angles of the slopes
 26 leading into the lake, we deem the possibility of a local sedimentary imprint as very low. This is supported by both XRF and

1 MS data. A thorough sedimentary analysis of potential sediment sources in the Glomma catchment could add valuable
2 information to the composition of the recorded flood deposits, and perhaps even denote source areas and thus also flood
3 triggering mechanisms of individual flood events (cf. Støren et al 2016). The 154450 km² size of the Glomma catchment, and
4 the mixing process involved, would however require a very large number of comparative samples. Moreover, The consistency
5 in bifurcation events causing peaks in concentration in both $Ti_{total\ scatter}$ and $K_{total\ scatter}$, as well as MS, suggests that the source
6 region for this signal remains the same throughout the record. The most likely source is thus the abundant glaciofluvial material
7 available in the area between Tarven and Flyginnsjøen (see Fig. 4).

8 A second assumption ~~is that~~ is that the river channel and landscape geometry controlling the bifurcation events has
9 not changed over the approximately recent 10 000 years to the extent that it alters this interplay between a flooding Glomma
10 and the investigated lake. The current river geometry was shaped by a glacial lake outburst flood (GLOF) some 10 000 -
11 10 4500 years ago with a peak discharge of more than 10^6 m³/s (Høgaas and Longva, 2016). This GLOF flushed the valley
12 where Glomma runs and also established the current river channel at Kongsvinger (Pettersson, 2000). Based on ~~(Klæboe,~~
13 ~~(1946) and (Hegge; (1968),~~ the threshold between Vingersjøen and Flyginnsjøen (Fig. 4) is a resilient and stable topographic
14 feature. The intermittent drainage patterns that route water from Vingersjøen to Flyginnsjøen during the bifurcation events
15 may have undergone some changes during the course of time, but it's hard to see how this would directly influence the
16 deposition of flood-delivered sediments to Flyginnsjøen. According to ~~(Hegge; (1968),~~ the flood events that occurred in 1967
17 CE and 1968 CE caused some erosion at the very highest elevation of this intermittent water course. Having said that, these
18 flood events did not cause any major damages to this area (Klæboe, 1946). In recent years, denser vegetation and also the
19 construction of a road bridge has potentially lessened the transfer capacity between the lakes although we have little or no
20 evidence for this based on what we observe in the lake core.

21 The resolution of the XRF signal is on average sub-annually, but because the uncertainty in the age-depth we
22 calculated flood rates, ~~i.e. average number of flood events,~~ for a moving 50 years window. Unlike the findings of Evin et al.,
23 (2019), and a Although the floods are of varying magnitude, there appears to be no systematic relationship between flood sizes
24 and, for instance, sediment thickness or volume except for the and flood sizes with the exception of Stor-Ofsen event. This is
25 probably explained by the fact that the sediment transport for individual floods will in part be deposited in the two preceding
26 lakes (Vingersjøen and Tarven) buffering Flyginnsjøen (Fig. 4), but may also indicate that event-specific features such as
27 ground frost or snow cover may regulate sediment availability.

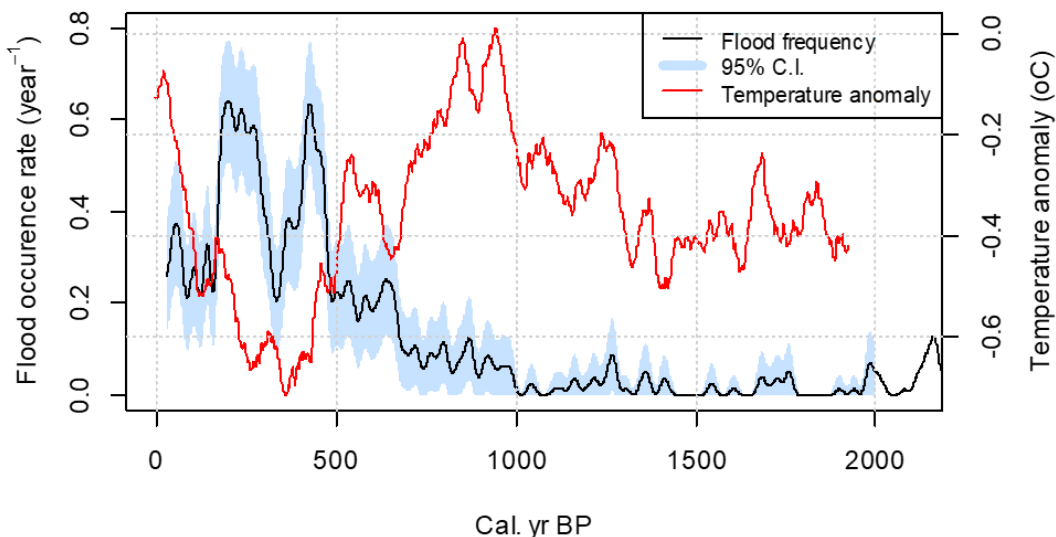
29 **5.2 Non-stationarity in flood records and regional climate co-variability**

30 The paleoflood data presented here document that the flood frequency is non-stationary during the last 10 300 years being
31 manifested on multiple time scales (Fig. 13). Non-stationarity is typically identified as quasi cyclic flood-rich and flood-poor
32 periods (for European studies, see e.g. Brázdil et al., 2005; Glaser et al., 2010; Hall et al., 2014; Jacobeit et al., 2003;
33 Kundzewicz and International Association of Hydrological Sciences., 2012; Mudelsee et al., 2004; Swierczynski et al., 2013)
34 where the flood rich period may last for 50-60 years (e.g. Glaser et al., 2010).

35 Over the instrumental, and the historical periodera, floods in the Glomma catchment have mainly occurred late in late
36 spring (late May, early June) as a result of due to the presence of large snow reservoirs that suddenly starts to due to the sudden
37 melting of large snow reservoirs -due to- a following a steep rise in temperatures that often ecombinedoverlaps with persistent
38 rain (Roald, 2013). Key processes that for Under the current climate conditions, generate the largest floods in the Glomma
39 catchment are caused by (i) high winter precipitation and preferentially lowcold winters temperatures resulting in a large snow
40 storage (ii) a cold spring followed by a sudden increase in air temperature typically resulting in producing high melt rates and
41 (iii) large amounts of widespread precipitation combined with snow melt (Vormoor et al., 2016). Importantly, for these spring-
42 snowmelt triggered floods, the soils are either frozen and/or already saturated with moisture channeling shallow sub-surface

1 flow and overland flow most waters to or shallow sub-surface flow or overland flows resulting in a fast discharge response to
2 snowmelt water and rain. Based on this knowledge these observations, we hypothesize that on decadal to centennial time scales,
3 increasing flood sizes can be explained by increasing precipitation, in particular during winter and spring, and decreasing cool
4 winter temperatures. Increasing spring and summer temperatures might potentially lead to increasing flood sizes, but this effect
5 depends strongly on the snow storage available for melt. Over the instrumental, and historic period floods in the Glomma
6 catchment have occurred late in spring (late May, early June) due to the presence of large snow reservoirs that suddenly starts
7 to melt due to a rise in temperatures often combined with persistent rain (Roald, 2013). The size of the spring flood depends
8 on the total snow accumulation during winter, that is controlled by both temperature and winter precipitation. Importantly, for
9 these spring snowmelt triggered floods, the soils are either frozen and/or already saturated with moisture channeling most
10 waters to or shallow sub-surface flow or overland flows resulting in a fast response to meltwater and rain.

11 In Figure 17 and 18 we compare the flood frequency reconstruction from Flyginnsjøen to several climate
12 reconstruction representing temperature and precipitation on a Comparing centennial to decadal scale variability. In the flood
13 frequency reconstruction from Flyginnsjøen with In Figure 17, the flood frequency is compared to regional summer
14 temperature reconstructions (Moberg et al., 2005), whereas in Figure 18 it is compared to (Fig. 17) and local records of glacier
15 variability (upper panel), a flood index (second panel) and local July temperature (third panel) in Figure 18. No reconstructions
16 of winter temperatures are available, and we assumed that the variations in summer temperatures to a large degree, reflect the
17 variations in winter temperatures. —No continuous reconstructions of winter precipitation are available for this region,
18 however, the glacier growth which in Scandinavia is primarily driven by summer temperatures and winter precipitation, and
19 the reconstructed flood record is therefore compared to glacier variability in Rondane in the upper Glomma catchment. - Low
20 values of the flood index from produced by Støren et al (2012) reflects periods with relatively high flood frequency in eastern
21 Norway. —We observe co-variability between the reconstructed flood frequency in Flyginnsjøen and several of the climate
22 reconstructions e variability which may indicate that the non-stationarity of flood frequency is, to a large degree, related to
23 non-stationarities in climate. The data from Flyginnsjøen shows, for instance, two distinct intervals with high flood frequency
24 during the ‘Little Ice Age’ (LIA), both played out on centennial time scales. — During this period the average summer
25 temperature for the northern hemisphere did not change substantially. The dip in flood frequency around year 400 BP might
26 be explained by other climate variables like winter precipitation. —Since 1850 there’s been a steady increase in summer
27 temperature followed by a reduction in flood frequency. Enhanced flooding during the LIA is observed in other lake studies
28 from eastern Norway as well, including Atnasjø (Nesje et al., 2001), Butjønnå (Bøe et al., 2006), Meringdalsvannet (Støren et
29 al., 2010) and also the river Grimsa in the headwater of Glomma (Killingland, 2009).



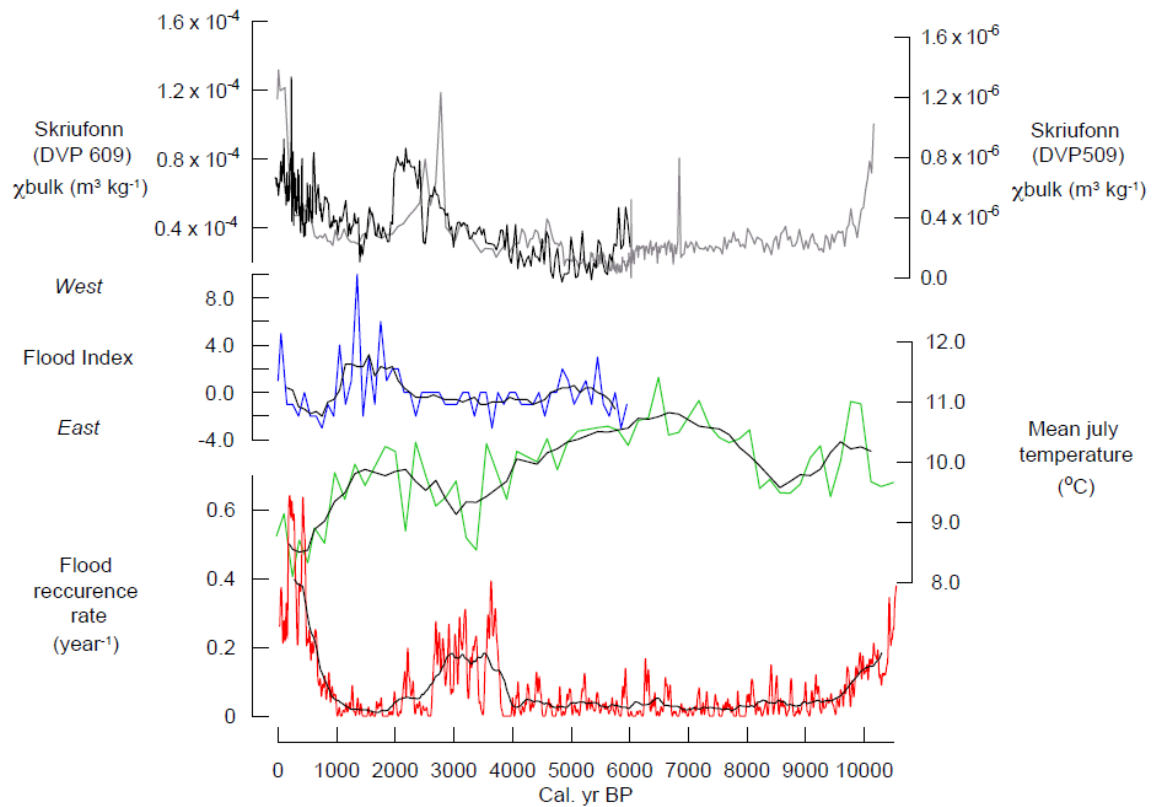
31

1 Figure 17: Flood frequency in Glomma (blue bars) and 30 years moving average Northern Hemisphere summer temperature
2 anomaly from Moberg et al. (20045).

3
4 Another period with heightened flood activity occurs roughly between 4000 to 2000 years ago. The increase in flood frequency
5 in Glomma during this period, and also during the LIA interval, coincides with a recorded decrease in summer temperature at
6 Bruscardstjørni in eastern Jotunheimen (Velle et al., 2010) and increasing glacier growth in Rondane (Kvisvik et al., 2015),
7 the mountainous source area of Glomma (Fig. 18). Multi-decadal periods are typical superimposed on centennial trends, as is
8 the case for both these two flood rich intervals. The near absence of floods prior to 4000 years ago is another recurring feature
9 in all flood records from Eastern Norway (e.g., Støren et al., 2016). Locally, it seems plausible that the effect of raising the 0-
10 isotherm with 100-300 m altitude, the effect of a warmer summer season, will significantly change the potential storage of
11 snow (Støren & Paasche, 2014).

12 ~~Over the instrumental, and historic period floods in the Glomma catchment have occurred late in spring (late May,~~
13 ~~early June) due to the presence of large snow reservoirs that suddenly starts to melt due to a rise in temperatures often combined~~
14 ~~with persistent rain (Roald, 2013). The size of the spring flood depends on the total snow accumulation during winter, that is~~
15 ~~controlled by both temperature and winter precipitation. Importantly, for these spring snowmelt triggered floods, the soils are~~
16 ~~either frozen and/or already saturated with moisture channeling most waters to or shallow sub-surface flow or overland flows~~
17 ~~resulting in a fast response to meltwater and rain.~~ The observed changes in flood frequency occurring both during the LIA and
18 in the first half of what sometimes is called the Neoglacial era (4000-2000 years ago) can thus, at least partially, be explained
19 by the combined effect of these flood generating processes (cf. Vormoor et al., 2016). The near-absence of floods prior to the
20 onset of the Neoglacial, when summer temperatures were ca 1°C higher than today (Velle et al., 2010), may be a valuable
21 albeit imperfect analogue for the coming century. During this period the 200-years flood is around 30% lower than today (Fig.
22 16).

23 In large catchments where snow melt is the primary flood generating process, it is suggested that we will may see smaller
24 flood sizes for easter Norway according to Lawrence (2020). In Lawrence (2020) a future climate in eastern Norway is suggest
25 that smaller flood sizes might be expected in large catchments where snow melt is the primary flood generating process. For
26 small catchment, in western Norway, where rain-generated floods already dominate, floods are expected to increase. Cooler
27 temperatures, especially in summer and spring are likely to delay the melting of the snow-cover – a scenario which enhances
28 increasing the probability for a sudden warming simply because it occurs later in the season.



1
 2 Figure 18: Flood frequency in Glomma (red) with 500yr running average, reconstructed summer temperature from
 3 Brurskardtjørni, southern Norway (Velle et al., 2010) (green) with 5-point running average, Flood index (blue) with 5-point
 4 running average (Støren et al., 2012) showing relative distribution of flood recurrence rate over southern Norway. Glacier
 5 activity at Skriufonn, Rondane southern Norway (Kvisvik et al., 2015) (Black and purple)

6
 7 The increase in flood frequency commencing at c. 4000 yr BP is a reoccurring feature not only in Europe but also in
 8 parts of the USA (Paasche and Støren, 2014). This hints at a large-scale change in the climate system at the time, with
 9 implications for both atmospheric circulation patterns and temperature trends. This major climate shift recorded in Europe is
 10 noteworthy because the flood seasonality is different across such a large area for many reasons, including the varying altitudinal
 11 differences. In high-lying areas in Austria (north of the Alps, Swierczynski et al., 2013), and in the and in the Central Alps
 12 (Switzerland and northern Italy, Wirth et al., 2013) floods start to increase, as in eastern Norway, rapidly just after 4000 years
 13 ago and remain on average high until 2000 years ago. Studying the relative distribution of floods in Norway, Støren et al.
 14 (2012) suggest that the long-term trends in the floods is dependent on changes in the distribution of winter precipitation related
 15 to semi-permanent shifts in atmospheric circulation patterns, and that an anomalous strong meridional component in the
 16 atmospheric circulation pattern are linked to floods in eastern Norway. Over the time period between the two flood rich periods
 17 in Glomma (c. 2000-1000 yr BP), Støren et al. (2012) recorded a westward shift in the flood frequency likely caused by reduced
 18 precipitation in the eastern areas (Fig. 18).

19 There are also potential catchment feedback mechanisms, not necessarily related to climate, that can both dampen
 20 and boost the flood patterns. The humanHumans can potentially influence on the landscape by forest clearing which would
 21 alter sediment availability and run-off patterns as well as change the overall buffering capacity.
 22 is a mechanism that potentially has a two fold impact on the flood patterns detected in the sediment core by changing the
 23 sediment availability in the catchment as well as theand the buffering capacity and hence the flood sizes. The 2500-4000-yr
 24 BP-flood-rich period occurring between 2500-4000 yr BP coincidence largely with the bronze age (2500-3700 BP) when
 25 settlements and farming expanded in Norway (REF?), but whether this early colonization impacted flood patterns remains an
 26 open question. Its worthwhile noticing that this interval with increased flooding is also recorded The increase in flood

1 frequency over this period coincide with flood rich periods in other lake sediment records from Southern Norway (Storen et
2 al., 2010; Bøe et al., 2006) as well as the observed shift in distribution of floods in Southern Norway which was only marginally
3 impacted by human activity if at all (shown in Fig. 18) arguably unaffected. We see, however, similar flood rich period in other
4 lake sediment records that certainly not are influenced by farming (shown in Fig. 18). We therefore argue that the effect of
5 land-use cannot be the main explanation ~~explain~~ for the observed changes in flood frequency during this period. A similar
6 conclusion was reached by Shubert et al., (2020), who show that logging and agricultural activities around lake Mondsee,
7 Austria, was low during flood rich periods, and that the flood record reflects climate variability rather than human activity in
8 the catchment.

9 In more recent times, ~~D~~eforestation is, for instance, ~~an~~ a candidate ~~additional explanation for~~ that potentially could
10 help explain the increase in flood frequency after ~~AD-1600 CE~~. The mining industry that started in Norway in the late 16th
11 century required a large amount of timber which resulted in widespread deforestation ~~also upper~~ in Glomma's ~~upper~~ catchment.
12 This removal of woodland cover may have influenced the local erosion and sediment transport of the upstream Glomma
13 catchment, but because this is area represents only a fraction of the total catchment area, we think that these 'excess sediments'
14 would be diluted downstream. Another relevant point here is that the flat downstream gradient of the river Glomma, potentially
15 causing sediment deposition long before they reach the bifurcation point at Kongsvinger. A final point ~~here~~ is that the sediment
16 source for the flood layers deposited in Flyginnsjøen is suggested to be mainly local, and the area around the lake and the
17 location for the bifurcation events itself was not subject to removal of woodland in this period ~~for~~. It is possible that the removal
18 of woodland amplified the size (and frequency) of floods since forests, in most cases, reduces flood peaks. This, however,
19 require a more regional and systematic vegetation change than that related to mining in the upper Glomma catchment to affect
20 the 154450 km² large catchment. ~~Some of these mechanisms discussed above could potential help explain why Stor-Ofsen in~~
21 ~~1789 is the largest local flood on record. As mentioned above, this~~ flood deposited the thickest sediment layer in the entire
22 record from Flyginnsjøen. The anomalous sediment thickness is also recorded in lake sediment archives for other places in
23 eastern Norway (see Bøe et al., 2006). Another amplifying process that can make floods become larger, and also remobilizing
24 lager amount of sediments, as ~~was~~ is the case for *Stor-Ofsen*, was the large number of upstream landslides that took place at
25 the time (Roald, 2013). In fact, the summer of 1789 was named 'skriusommaren' (the landslide summer) in historical material
26 (Roald, 2013). ~~We note that some of these historical slides might have occurred shortly after the flood as well.~~

27 ~~Deforestation is, for instance, an additional explanation for the increase in flood frequency after AD 1600. The mining~~
28 ~~industry that started in Norway in the 16th century required a large amount of timber which resulted in widespread deforestation~~
29 ~~also in Glomma's catchment. Some of these mechanisms could potential help explain why Stor Ofsen in 1789 is the largest~~
30 ~~local flood on record. As mentioned above, the flood deposited the thickest sediment layer in the entire record from~~
31 ~~Flyginnsjøen. The anomalous sediment thickness is also recorded in lake sediment archives for other places in eastern Norway~~
32 ~~(see Bøe et al., 2006). Another amplifying process that can make floods become larger, and also remobilizing lager amount of~~
33 ~~sediments, as was the case for Stor Ofsen, was the large number of upstream landslides that took place at the time (Roald,~~
34 ~~2013). In fact, the summer of 1789 was named 'skriusommaren' (the landslide summer) in historical material (Roald, 2013).~~
35 ~~We note that some of these historical slides might have occurred shortly after the flood as well.~~

37 5.3 Flood quantile estimation by combining systematic-, historical- and paleoflood data

38 The non-stationarity in flood frequency is a major challenge when estimating flood quantiles used for land planning and design
39 of infrastructure given that one needs to predict how the flood frequency will evolve over the life time of the construction, e.g.
40 for bridges it is 100 years (Koh et al., 2014). Milly et al. (2008) argued that 'stationarity is dead' and that it is necessary to
41 account for non-stationarity in order to avoid under-estimation of risks based on design floods.

1 Conversely, Serinaldi and Kilsby (2015) posited that ‘stationarity is undead’ because a stationary model is robust and
2 can be a useful reference/benchmark. Accounting for uncertainty in a stationary model can be as important as including non-
3 stationarity within a risk assessment framework. A non-stationary model introduces more parameters and thereby, in most
4 cases, increases the estimation uncertainty. An additional challenge when applying a non-stationary model for design flood
5 estimation is to project the flood frequency into the future.

6 The paleoflood data presented here suggests that the flood frequency is non-stationary and that there is indeed flood
7 rich and flood poor periods (Fig. 13). Since design flood estimates are used for assessing average risk over the lifetime of a
8 construction, it is desired that design flood estimates are stable over time and not sensitive to quasi cyclic variations in flood
9 sizes on annual to decadal time scales. It is, however, important to account for trends or shifts in flood frequency. Macdonald
10 et al. (2014) show that on centennial time scales, the effect of cyclic variations in short systematic records can effectively be
11 removed by a temporal extension of flood time series using historical information. Data from Flyginnsjøen and historical data
12 reveals that a quasi-stationary period can be identified at centennial time scales, but not on a sub-millennium time scale where
13 major shifts in flood frequency are identified (Fig. 13).

14 In this study, we firstly used the stationarity assumption and evaluated several possible ways to combine the three
15 data sources within a stationary framework. The results in Fig. 14 and 15 show that the design flood estimates are sensitive to
16 how we combine the systematic, historical and paleo flood data. We used 65 years of systematic data covering the period ~~AD~~
17 ~~CE~~ 1872 – 1936 for which we assume that the effect of river regulation is negligible. Adding the historical data from the flood
18 stone covering the period from ~~AD-CE~~ ~~165375~~ to 1871, substantially increased the estimates of the flood quantiles and slightly
19 reduced the estimation uncertainty (Fig. 14).

20 The paleoflood timeseries provided here suggests that the flood frequency during the historical period is non-
21 stationary where the 18th century was an extremely flood rich period (Fig. 13), and that the ~~AD-CE~~ 1789 flood was an
22 exceptional flood during the 10 300 years covered by the sediment core. Based on this paleo-information, we used historical
23 data from the 19th century, and added the ~~AD-CE~~ 1789 flood by assuming it was the largest flood over a period of 10 300
24 years. This slightly reduced the flood quantile estimates as compared to using all historical information and substantially
25 reduced the estimation uncertainty (Fig. 14). These results shows that for the site at Elverum, we should be careful when
26 including historical flood information from the flood rich period in the 18th century.

27 As a next step, we added the paleo-flood data ~~representing for the recent 572600~~ years (i.e. ~~CE~~ 1300-1871-~~CE~~). This
28 resulted in negligible differences in flood quantile and uncertainty estimates (Fig. 15) indicating that the information content
29 in the paleodata alone can be small. A possible explanation is the combination of the relatively low threshold (according to
30 Fig. 15 it is around a 5-years flood), and that we only had information about the number of flood events. Both Macdonald et
31 al. (2014)- and Engeland et al. (2018) show that the information content is low when the threshold for historical floods ~~isare~~
32 too low.

33 In a final step we used the flood rate from the sediment core as a key to explore non-stationarity of the design flood
34 estimates, exemplified by the 200-years flood (Fig. 16). We could see important variation during the recent 6000 years. The
35 200 years flood was estimated to be around 23 % higher during the flood rich periods in the 18th century and 20% lower during
36 the warmest period. The high values for the 200-years flood during the 18th century is confirmed by the historical data. This
37 variation in design floods is, interestingly within the range seen in recent studies on climate change impacts on floods in
38 Norway (Lawrence, 2020). For a future climate that is expected to be warmer, the design flood might be expected to decrease.
39 Furthermore, this shows that the most interesting information we could get from the sediment core was the non-stationarity in
40 floods.

1 **6.0 Conclusions**

2 In this study we have (i) compiled historical flood data from existing literature, (ii) presented an analysis of sediment core
3 extracted from the lake Flyginnsjøen in Norway including results of XRF- and CT-scans plus MS measurements and used
4 these data to estimate flood frequency over a period of 10 300 years, and (iii) combined flood data from systematic streamflow
5 measurements, historical sources and lacustrine sediment cores for estimating design floods and assessing non-stationarities
6 in flood frequency at Elverum in the Glomma catchment located in eastern Norway. Our results show that

- 8 • Based on detailed analysis of lake sediments that trap sediments whenever the river Glomma exceeds a local
9 threshold, we could estimate flood frequency in a moving window of 50 years throughout the last 10 300 years.
- 10 • The paleodata shows that the flood frequency is non-stationary across time scales. Flood rich periods has been
11 identified, and these periods corresponds well to similar data in eastern Norway and also in the Alps such as the
12 increase around 4000 years ago. The flood frequency can show significant non-stationarities within a flood rich
13 period. The most recent period with a high flood frequency was the 18th century, and the 1789 flood (*Stor-Ofsen*) is
14 probably the largest flood during the entire Holocene.
- 15 • The estimation of flood quantiles benefits from the use of historical and paleo data. The paleodata were in particular
16 useful for evaluating the historical data. We identified that the 1789 flood was the largest one for the recent 10 300
17 years and that the 18th century was a flood rich period as compared to the 20th and 19th centuries. Using the frequency
18 of floods obtained from the paleo-flood record resulted in minor changes in design flood estimates.
- 19 • We could use the paleodata to explore non-stationarity in design flood estimates. During the coldest period in the 18th
20 century, the design flood was up to 23 % higher than today, and down to 30% lower in a warmer climate c. 4000-
21 6000 years ago.

22
23 This study has demonstrated the usefulness of paleo-flood data and we suggest that paleodata has a high potential for detecting
24 links between climate dynamics and flood frequency. The data presented in this study could be used alone, or in combination
25 with paleo-flood data from other locations in Norway and Europe, to analyze the links between changes in climate and its
26 variability and flood frequency.

27 **Data availability**

28 Systematic flood data are available from the national hydrological database at the Norwegian Water Resources and Energy
29 Directorate. The data from the scanning of the sediment cores are available upon request to the authors.

30 **Author contribution**

31 The study was designed and planned by AA, KE, IS and ES. IS and ES carried out the lake coring and the field work. AA, IS,
32 ØP, and ES all contributed the scanning and analysis if the sediment cores. AA, KE and ES contributed to systematization of
33 historical and systematic flood data and the flood frequency analysis. AA prepared Figure 1 and 3 ES and ØP prepared Figure
34 4. ES prepared Figure 5-, 9, 10, 11 and 18. KE prepared Figure 2, 6, 7, 8, 12, 13, 14, 15, 16, and 17. KE prepared the manuscript
35 with contribution from all co-authors.

36 **Competing interests**

37 The authors declare that they have no conflict of interest.

38

1 **Acknowledgement**

2 We would like to extend our thanks to Svein Olaf Dahl, Nils Roar Sæltun and Chong-Yu Xu who co-supervised the master
3 projects of IS (Dept. of Geogaphy, UiB) and AA (Dept. of Geoscience, UiO) that create the basis for this study, and Karoline
4 Follestand and Martin Tvedt who assisted in coring lake Flyginnsjøen. This study became part of the Hordafloam project which
5 is funded by RFF-Vest, Hordaland County. ØP acknowledges the project ACER (812957), funded by Research Council of
6 Norway. All core samples, apart from the dating, were measured at the Earth Surface Sediment Laboratory (EARTHLAB)
7 (226171) at Department of Earth Science, University of Bergen.

8

9 **7.0 References**

- 10 Aano, A.: Flood frequency analyses based on streamflow time series, historical information and paleohydrological data., 2017.
- 11 Alfieri, L., Bisselink, B., Dottori, F., Naumann, G., de Roo, A., Salamon, P., Wyser, K. and Feyen, L.: Global projections of
12 river flood risk in a warmer world, *Earth's Future*, 5(2), 171–182, doi:10.1002/2016EF000485, 2017.
- 13 Appleby, P. G.: Chronostratigraphic Techniques in Recent Sediments, in *Tracking Environmental Change Using Lake*
14 *Sediments*, pp. 171–203, Kluwer Academic Publishers., 2001.
- 15 Appleby, P. G. and Piliposian, G. T.: Radiometric Dating of Lake Sediment Cores from Flyginnsjøen and Vingersjøen,
16 Southern Norway (provisional report), Liverpool., 2014.
- 17 Baker, V. R.: Paleohydrology and sedimentology of lake missoula flooding in Eastern Washington, Special Paper of the
18 Geological Society of America, 144, 1–73, doi:10.1130/SPE144-p1, 1973.
- 19 Baker, V. R.: Paleoflood hydrology and extraordinary flood events, *Journal of Hydrology*, 96(1–4), 79–99, doi:10.1016/0022-
20 1694(87)90145-4, 1987.
- 21 Baker, V. R.: Paleoflood hydrology: Origin, progress, prospects, *Geomorphology*, 101(1–2), 1–13,
22 doi:10.1016/j.geomorph.2008.05.016, 2008.
- 23 Benito, G. and O'Connor, J. E.: Quantitative Paleoflood Hydrology, in *Treatise on Geomorphology*, vol. 9, pp. 459–474.,
24 2013.
- 25 Benito, G. and Thorndycraft, V. R.: Palaeoflood hydrology and its role in applied hydrological sciences, *Journal of Hydrology*,
26 313(1–2), 3–15, doi:10.1016/j.jhydrol.2005.02.002, 2005.
- 27 Benito, G., Brázdil, R., Herget, J. and Machado, M. J.: Quantitative historical hydrology in Europe, *Hydrology and Earth*
28 *System Sciences*, 19(8), 3517–3539, doi:10.5194/hess-19-3517-2015, 2015.
- 29 Benson, M. A.: Use of historical data in flood-frequency analysis, *Eos, Transactions American Geophysical Union*, 31(3),
30 419–424, doi:10.1029/TR031i003p00419, 1950.
- 31 Blaauw, M. and Christeny, J. A.: Flexible paleoclimate age-depth models using an autoregressive gamma process, *Bayesian*
32 *Analysis*, 6(3), 457–474, doi:10.1214/11-BA618, 2011.
- 33 Blake, G. R. and Hartge, K. H.: Bulk Density, in *Methods of Soil Analysis: Part 1—Physical and Mineralogical Methods*,
34 edited by K. A, pp. 363–375, American Society of Agronomy-Soil Science Society of America, Madison., 1986.
- 35 Blöschl, G., Hall, J., Parajka, J., Perdigão, R. A. P., Merz, B., Arheimer, B., Aronica, G. T., Bilibashi, A., Bonacci, O., Borga,
36 M., Čanjevac, I., Castellarin, A., Chirico, G. B., Claps, P., Fiala, K., Frolova, N., Gorbachova, L., Gül, A., Hannaford, J.,

- 1 Harrigan, S., Kireeva, M., Kiss, A., Kjeldsen, T. R., Kohnová, S., Koskela, J. J., Ledvinka, O., Macdonald, N., Mavrova-
2 Guirguinova, M., Mediero, L., Merz, R., Molnar, P., Montanari, A., Murphy, C., Osuch, M., Ovcharuk, V., Radevski, I.,
3 Rogger, M., Salinas, J. L., Sauquet, E., Šraj, M., Szolgay, J., Viglione, A., Volpi, E., Wilson, D., Zaimi, K. and Živković, N.:
4 Changing climate shifts timing of European floods, *Science*, 357(6351), 588–590, doi:10.1126/science.aan2506, 2017.
- 5 Blöschl, G., Hall, J., Viglione, A., Perdigão, R. A. P., Parajka, J., Merz, B., Lun, D., Arheimer, B., Aronica, G. T., Bilibashi,
6 A., Boháč, M., Bonacci, O., Borga, M., Čanjevac, I., Castellarin, A., Chirico, G. B., Claps, P., Frolova, N., Ganora, D.,
7 Gorbachova, L., Gül, A., Hannaford, J., Harrigan, S., Kireeva, M., Kiss, A., Kjeldsen, T. R., Kohnová, S., Koskela, J. J.,
8 Ledvinka, O., Macdonald, N., Mavrova-Guirguinova, M., Mediero, L., Merz, R., Molnar, P., Montanari, A., Murphy, C.,
9 Osuch, M., Ovcharuk, V., Radevski, I., Salinas, J. L., Sauquet, E., Šraj, M., Szolgay, J., Volpi, E., Wilson, D., Zaimi, K. and
10 Živković, N.: Changing climate both increases and decreases European river floods, *Nature*, 573(7772), 108–111,
11 doi:10.1038/s41586-019-1495-6, 2019.
- 12 Bøe, A.-G., Dahl, S. O., Lie, Ø. and Nesje, A.: Holocene river floods in the upper Glomma catchment, southern Norway: a
13 high-resolution multiproxy record from lacustrine sediments, *The Holocene*, 16, 445–455, doi:10.1191/0959683606hl940rp,
14 2006.
- 15 Brázdil, R., Pfister, C., Wanner, H., von Storch, H. and Luterbacher, J.: Historical climatology in Europe - The state of the art,
16 *Climatic Change*, 70(3), 363–430, doi:10.1007/s10584-005-5924-1, 2005.
- 17 Brázdil, R., Kundzewicz, Z. W. and Benito, G.: Historical hydrology for studying flood risk in Europe, *Hydrological Sciences*
18 *Journal*, 51(5), 739–764, doi:10.1623/hysj.51.5.739, 2006a.
- 19 Brázdil, R., Kundzewicz, Z. W. and Benito, G.: Historical hydrology for studying flood risk in Europe, *Hydrological Sciences*
20 *Journal*, 51(5), 739–764, doi:10.1623/hysj.51.5.739, 2006b.
- 21 Brázdil, R., Máčka, Z., Řezníčková, L., Soukalová, E., Dobrovolný, P. and Grygar, T. M.: Floods and floodplain changes of
22 the River Morava, the Strážnické Pomoraví region (Czech Republic) over the past 130 years, *Hydrological Sciences Journal*,
23 56(7), 1166–1185, doi:10.1080/02626667.2011.608359, 2011.
- 24 Brázdil, R., Kundzewicz, Z. W., Benito, G., Demarée, G., Macdonald, N. and Roald, L. A.: Historical floods in Europe in the
25 past millennium, IAHS-AISH Publication, (SPEC. ISS. 10), 121–166, doi:10.1201/b12348-7, 2012.
- 26 Bretz, J. H.: Valley Deposits Immediately East of the Channeled Scabland of Washington. I, *The Journal of Geology*, 37, 393–
27 427, doi:10.2307/30056651, 1929.
- 28 Coles, S. G. and Dixon, M. J.: Likelihood-Based Inference for Extreme Value Models, *Extremes*, 2(1), 5–23,
29 doi:10.1023/A:1009905222644, 1999.
- 30 [Cunnane, C. Unbiased plotting positions – a review – comments. *Journal of Hydrology* 37, 205–222. doi:10.1016/0022-](#)
31 [1694\(78\)90017-3, 1978](#)
- 32 Czymzik, M., Brauer, A., Dulski, P., Plessen, B., Naumann, R., von Grafenstein, U. and Scheffler, R.: Orbital and solar forcing
33 of shifts in Mid- to Late Holocene flood intensity from varved sediments of pre-alpine Lake Ammersee (southern Germany),
34 *Quaternary Science Reviews*, 61, 96–110, doi:10.1016/j.quascirev.2012.11.010, 2013.
- 35 Dana, J. D.: The flood of the Connecticut River valley from the melting of the Quaternary glacier, *American Journal of Science*,
36 s3-23(134), 87–97, doi:10.2475/ajs.s3-23.134.87, 1882.
- 37 Dean, W. E. Jr.: Determination of Carbonate and Organic Matter in Calcareous Sediments and Sedimentary Rocks by Loss on
38 Ignition: Comparison With Other Methods, *SEPM Journal of Sedimentary Research*, Vol. 44(1), 242–248,
39 doi:10.1306/74d729d2-2b21-11d7-8648000102c1865d, 1974.

- 1 Debret, M., Chapron, E., Desmet, M., Rolland-Revel, M., Magand, O., Trentesaux, A., Bout-Roumazielle, V., Nomade, J. and
2 Arnaud, F.: North western Alps Holocene paleohydrology recorded by flooding activity in Lake Le Bourget, France,
3 *Quaternary Science Reviews*, 29(17–18), 2185–2200, doi:10.1016/j.quascirev.2010.05.016, 2010.
- 4 Embrechts, P., Klüppelberg, C. and Mikosch, T.: *Modelling Extremal Events*, Springer Berlin Heidelberg, Berlin, Heidelberg.,
5 1997.
- 6 Engeland, K., Wilson, D., Borsányi, P., Roald, L. and Holmqvist, E.: Use of historical data in flood frequency analysis: A case
7 study for four catchments in Norway, in *Hydrology Research*, vol. 49, pp. 466–486, Nordic Association for Hydrology., 2018.
- 8 [Evin, G., Wilhelm B., Jenny J.P.: Flood hazard assessment of the Rhône River revisited with reconstructed discharges from
9 lake sediments. *Global and Planetary Change* 172 \(114-123\) , , 10.1016/j.gloplacha.2018.09.010, 2019](#)
- 10 Finne-Grønn, S. H.: Elverum : en bygdebeskrivelse. 2 : Bygdens almindelige historie, institutioner og embedsmænd,
11 Cammenmeyers Boghandel, Oslo. [online] Available from:
12 <https://www.nb.no/items/0c92bf63bcd34a40d851ec9aed2d8f07?page=243&searchText=elverum%20en%20bygdebeskrivelse>
13 e (Accessed 5 March 2020), 1921.
- 14 Fisher, R. A. and Tippett, L. H. C.: Limiting forms of the frequency distribution of the largest or smallest member of a sample,
15 *Mathematical Proceedings of the Cambridge Philosophical Society*, 24(02), 180–190, doi:10.1017/S0305004100015681,
16 1928.
- 17 Follestad, K.: Reconstruction of floods in Glomma through the holos - Effects of climate change on different flood regimes
18 (Rekonstruksjon av flommer i Glomma gjennom holosen - Effekter av klimaendringer på ulike flomregimer - in Norwegian),
19 Bergen. [online] Available from: [https://www.uib.no/geografi/83037/rekonstruksjon-av-flommer-i-glomma-gjennom-](https://www.uib.no/geografi/83037/rekonstruksjon-av-flommer-i-glomma-gjennom-holosen-effekter-av-klimaendringer-pa)
20 [holosen-effekter-av-klimaendringer-pa](https://www.uib.no/geografi/83037/rekonstruksjon-av-flommer-i-glomma-gjennom-holosen-effekter-av-klimaendringer-pa) (Accessed 5 March 2020), 2014.
- 21 Gaál, L., Szolgay, J., Kohnová, S., Hlavčová, K. and Viglione, A.: Inclusion of historical information in flood frequency
22 analysis using a Bayesian MCMC technique: a case study for the power dam Orlik, Czech Republic, *Contributions to*
23 *Geophysics and Geodesy*, 40, 121–147, doi:10.2478/v10126-010-0005-5, 2010.
- 24 Gilli, A., Anselmetti, F. S., Glur, L. and Wirth, S. B.: Lake Sediments as Archives of Recurrence Rates and Intensities of Past
25 Flood Events, in *Dating Torrential Processes on Fans and Cones*, vol. 47, edited by M. Schneuwly-Bollschweiler, M. Stoffe,
26 and F. Rudolf-Miklau, pp. 225–242, Springer International Publishing., 2013.
- 27 Glaser, R., Riemann, D., Schönbein, J., Barriendos, M., Brázdil, R., Bertolin, C., Camuffo, D., Deutsch, M., Dobrovolný, P.,
28 van Engelen, A., Enzi, S., Haličková, M., Koenig, S. J., Kotyza, O., Limanówka, D., Macková, J., Sghedoni, M., Martin, B.
29 and Himmelsbach, I.: The variability of European floods since AD 1500, *Climatic Change*, 101(1–2), 235–256,
30 doi:10.1007/s10584-010-9816-7, 2010.
- 31 GLB: *Glommen og Laagens Grukseierforening 1918-43*, Grøndahl & Sønns Boktrykkeri, Oslo., 1947.
- 32 Gnedenko, B.: Sur La Distribution Limite Du Terme Maximum D'Une Serie Aleatoire, *The Annals of Mathematics*, 44(3),
33 423, doi:10.2307/1968974, 1943.
- 34 Goslar, T.: *Poznan Radiocarbon Laboratory*, Poland, Poznan., 2014.
- 35 Grønlund, A., Njøs, A. and Kløve, B.: *Endringer i landbrukets arealbruk i Glommas nedbørfelt*, Oslo. [online] Available from:
36 <http://publikasjoner.nve.no/hydra/rapport/n02.pdf> (Accessed 5 March 2020), 1999.
- 37 Hall, J., Arheimer, B., Borga, M., Brázdil, R., Claps, P., Kiss, a., Kjeldsen, T. R., Kriaučiūnienė, J., Kundzewicz, Z. W., Lang,
38 M., Llasat, M. C., Macdonald, N., McIntyre, N., Mediero, L., Merz, B., Merz, R., Molnar, P., Montanari, a., Neuhold, C.,
39 Parajka, J., Perdigão, R. a. P., Plavcová, L., Rogger, M., Salinas, J. L., Sauquet, E., Schär, C., Szolgay, J., Viglione, a. and

- 1 Blöschl, G.: Understanding flood regime changes in Europe: a state-of-the-art assessment, *Hydrology and Earth System*
2 *Sciences*, 18(7), 2735–2772, doi:10.5194/hess-18-2735-2014, 2014.
- 3 Hanssen-Bauer, I. Førland, E. J. Haddeland, I., Hisdal, H., Lawrence, D., Mayer, S., Nesje, A., Sandven, J. E. Ø., Sandø, A.
4 B. and Sorteberg, A. Ådlandsvik, B.: *Climate in Norway 2100: a knowledge based for climate adaptation.*, 2017.
- 5 Hegge, K.: Glommas Bifurkasjon Ved Kongsvinger, *Norsk Geografisk Tidsskrift*, 22(2), 166–171,
6 doi:10.1080/00291956808551859, 1968.
- 7 Hegge, K.: Large floods in Glomma (Store flommer i Glomma - in Norwegian), , 2, 1969.
- 8 Hirabayashi, Y., Mahendran, R., Koirala, S., Konoshima, L., Yamazaki, D., Watanabe, S., Kim, H. and Kanae, S.: Global
9 flood risk under climate change, *Nature Climate Change*, 3(9), 816–821, doi:10.1038/nclimate1911, 2013.
- 10 [Hirsch, R. M. & Stedinger, J. R. Plotting positions for historical floods and their precision. *Water Resources Research* 23 \(4\),
11 715–727. doi:10.1029/WR023i004p00715, 1987](#)
- 12 Høgaas, F. and Longva, O.: Mega deposits and erosive features related to the glacial lake Nedre Glomsjø outburst flood,
13 southeastern Norway, *Quaternary Science Reviews*, 151, 273–291, doi:10.1016/j.quascirev.2016.09.015, 2016.
- 14 IPCC: *Managing the Risks of Extreme Events and Disasters to Advance Climate Change Adaptation* — IPCC, edited by C. B.
15 Field, V. Barros, T. F. Stocker, D. Qin, D. J. Dokken, K. L. Ebi, M. D. Mastrandrea, K. J. Mach, G.-K. Plattner, S. K. Allen,
16 M. Tignor, and P. M. Midgley, Cambridge University Press. [online] Available from: [https://www.ipcc.ch/report/managing-](https://www.ipcc.ch/report/managing-the-risks-of-extreme-events-and-disasters-to-advance-climate-change-adaptation/)
17 [the-risks-of-extreme-events-and-disasters-to-advance-climate-change-adaptation/](https://www.ipcc.ch/report/managing-the-risks-of-extreme-events-and-disasters-to-advance-climate-change-adaptation/) (Accessed 4 March 2020), 2012.
- 18 Jacobeit, J., Glaser, R., Luterbacher, J. and Wanner, H.: Links between flood events in central Europe since AD 1500 and
19 large-scale atmospheric circulation modes, *Geophysical Research Letters*, 30(4), 2–5, doi:10.1029/2002GL016433, 2003.
- 20 Killingland, K. E. N.: Extreme floods in Grimsa, upper Glomma. Reconstruction of flood frequency through holocene and
21 vulnerability analysis of today's river (Ekstremflommer i Grimsa, øvre Glommavassdraget Rekonstruksjon av flomfrekvens
22 gjennom holosen og sårbarhetsanalyse av d, The University of Bergen., 2009.
- 23 Kjeldsen, T. R., Macdonald, N., Lang, M., Mediero, L., Albuquerque, T., Bogdanowicz, E., Bra'zdl, R., Castellarin, A., David,
24 V., Fleig, A., Gu'l, G. O., Kriaciuniene, J., Kohnova', S., Merz, B., Nicholson, O., Roald, L. A., Salinas, J. L., Sarauskiene,
25 D., S'raj, M., Strupczewski, W., Szolgay, J., Toumazis, A., Vanneuville, W., Veijalainen, N. and Wilson, D.: Documentary
26 evidence of past floods in Europe and their utility in flood frequency estimation, *Journal of Hydrology*, 517, 963–973,
27 doi:10.1016/j.jhydrol.2014.06.038, 2014.
- 28 Klæboe, H.: Glommas bifurkasjon ved kongsvinger, *Norsk Geografisk Tidsskrift*, 11(5–6), 266–275,
29 doi:10.1080/00291954608551633, 1946.
- 30 Kochel, R. C. and Baker, V. R.: Paleoflood hydrology, *Science*, 215(4531), 353–361, doi:10.1126/science.215.4531.353, 1982.
- 31 Koh, H. M., Park, W. and Choo, J. F.: Lifetime design of long-span bridges, *Structure and Infrastructure Engineering*, 10(4),
32 521–533, doi:10.1080/15732479.2013.769013, 2014.
- 33 Kundzewicz, Zbigniew. and International Association of Hydrological Sciences.: *Changes in flood risk in Europe,*
34 *International Association of Hydrological Sciences.*, 2012.
- 35 Kvernmoen, G. T. and Kvernmoen, T.: *Flomopptegnelser (1740-1839)*, in *Elverum – en bygdebeskrivelse –II – Bygdens*
36 *almenne historie*», edited by S. H. Finne-Grønn, Oslo., 1921.
- 37 Kvisvik, B. C., Paasche, Ø. and Dahl, S. O.: Holocene cirque glacier activity in Rondane, southern Norway, *Geomorphology*,
38 246, 433–444, doi:10.1016/j.geomorph.2015.06.046, 2015.

- 1 Lawrence, D.: Uncertainty introduced by flood frequency analysis in projections for changes in flood magnitudes under a
2 future climate in Norway, *Journal of Hydrology: Regional Studies*, 28, 100675, doi:10.1016/j.ejrh.2020.100675, 2020.
- 3 Lovdata: Dam Safety Regulation (Forskrift om sikkerhet ved vassdragsanlegg, in Norwegian). [online] Available from:
4 <https://lovdata.no/dokument/SF/forskrift/2009-12-18-1600?q=damsikkerhet> (Accessed 5 March 2020), 2010.
- 5 Macdonald, N. and Sangster, H.: High-magnitude flooding across Britain since AD 1750, *Hydrology and Earth System
6 Sciences*, 21(3), 1631–1650, doi:10.5194/hess-21-1631-2017, 2017.
- 7 Macdonald, N., Kjeldsen, T. R., Prosdocimi, I. and Sangster, H.: Reassessing flood frequency for the Sussex Ouse, Lewes: the
8 inclusion of historical flood information since AD 1650, *Natural Hazards and Earth System Sciences*, 14(10), 2817–2828,
9 doi:10.5194/nhess-14-2817-2014, 2014.
- 10 Martins, E. S. and Stedinger, J. R.: Generalized maximum-likelihood generalized extreme-value quantile estimators for
11 hydrologic data, *Water Resources Research*, 36(3), 737–744, doi:10.1029/1999WR900330, 2000.
- 12 Martins, E. S. and Stedinger, J. R.: Historical information in a generalized maximum likelihood framework with partial
13 duration and annual maximum series, *Water Resources Research*, 37(10), 2559–2567, doi:10.1029/2000WR000009, 2001.
- 14 Milly, P. C. D., Betancourt, J., Falkenmark, M., Hirsch, R. M., Kundzewicz, Z. W., Lettenmaier, D. P. and Stouffer, R. J.:
15 Stationarity Is Dead: Whither Water Management?, *Science*, 319(5863), 573–574, doi:10.1126/science.1151915, 2008.
- 16 [Moberg, A., Sonechkin, D. M., Holmgren, K., Datsenko, M. H. and Karlén, W.: Highly variable Northern Hemisphere
17 temperatures reconstructed from low- and high-resolution proxy data, *Nature*, 433\(7026\), 613–617, doi:10.1038/nature03265,
18 2005.](#)
- 19 Mudelsee, M., Börngen, M., Tetzlaff, G. and Grünewald, U.: Extreme floods in central Europe over the past 500 years: Role
20 of cyclone pathway “Zugstrasse Vb,” *Journal of Geophysical Research D: Atmospheres*, 109(23), 1–21,
21 doi:10.1029/2004JD005034, 2004.
- 22 Nesje, A.: A piston corer for lacustrine and marine sediments, *Arctic and Alpine Research*, 24(3), 257–259,
23 doi:10.2307/1551667, 1992.
- 24 Nesje, A., Dahl, S. O., Matthews, J. A. and Berrisford, M. S.: A ~4500 yr record of river floods obtained from a sediment core
25 in Lake Atnsjøen, eastern Norway, *Journal of Paleolimnology*, 25(3), 329–342, doi:10.1023/A:1011197507174, 2001.
- 26 NVE flood zone maps: NVE flood zone maps, [online] Available from: <https://gis3.nve.no/link/?link=flomsone> (Accessed 23
27 May 2020), 2020.
- 28 Orvedal, K. and Peereboom, I. O.: Flood zone map Førde (Flaumsonkart Delprosjekt Førde - in Norwegian), 2014.
- 29 Otnes, J.: Old floodmarks at River Glomma (Gamle flommerker langs Glåma, Årbok for Glåmdalen 41, 6–26), Elverum Trykk,
30 Elverum., 1982.
- 31 Paasche, Ø. and Støren, E. W. N.: How Does Climate Impact Floods? Closing the Knowledge Gap, *Eos, Transactions
32 American Geophysical Union*, 95(28), 253–254, doi:10.1002/2014EO280001, 2014.
- 33 Payraastre, O., Gaume, E. and Andrieu, H.: Usefulness of historical information for flood frequency analyses: Developments
34 based on a case study, *Water Resources Research*, 47, doi:10.1029/2010WR009812, 2011.
- 35 Pettersson, L.-E.: Flood estimation for the Glomma river upstream Vormå (Flomberegning for Glommavassdraget oppstrøms
36 Vormå - in Norwegian), Oslo. [online] Available from: www.nve.no (Accessed 5 March 2020), 2000.
- 37 Pettersson, L.-E.: Glomma’s bifurcation at Kongsvinger (Glommas bifurkasjon ved Kongsvinger - in Norwegian), Oslo.
38 [online] Available from: www.nve.no (Accessed 5 March 2020), 2001.

- 1 Prodocimi, I.: German tanks and historical records: the estimation of the time coverage of ungauged extreme events,
2 Stochastic Environmental Research and Risk Assessment, 32(3), 607–622, doi:10.1007/s00477-017-1418-8, 2018.
- 3 Reimer, P. J., Bard, E., Bayliss, A., Beck, J. W., Blackwell, P. G., Ramsey, C. B., Buck, C. E., Cheng, H., Edwards, R. L.,
4 Friedrich, M., Grootes, P. M., Guilderson, T. P., Haflidason, H., Hajdas, I., Hatté, C., Heaton, T. J., Hoffmann, D. L., Hogg,
5 A. G., Hughen, K. A., Kaiser, K. F., Kromer, B., Manning, S. W., Niu, M., Reimer, R. W., Richards, D. A., Scott, E. M.,
6 Southon, J. R., Staff, R. A., Turney, C. S. M. and van der Plicht, J.: IntCal13 and Marine13 Radiocarbon Age Calibration
7 Curves 0–50,000 Years cal BP, Radiocarbon, 55(4), 1869–1887, doi:10.2458/azu_js_rc.55.16947, 2013.
- 8 Renard, B., Sun, X. and Lang, M.: Bayesian Methods for Non-stationary Extreme Value Analysis, pp. 39–95., 2013.
- 9 Renberg, I. and Hansson, H.: The HTH sediment corer, Journal of Paleolimnology, 40(2), 655–659, doi:10.1007/s10933-007-
10 9188-9, 2008.
- 11 Reusch, H.: Glomma's bend at Kongsvinger (Glommens bøining ved Kongsvinger), in Norges Geografiske Selskab, Aarbog,
12 14, pp. 96–102., 1903.
- 13 Roald, L.: Floods in Norway (Flom i Norge - in Norwegian), Forlaget Tom & Tom, Oslo., 2013.
- 14 Schendel, T. and Thongwichian, R.: Considering historical flood events in flood frequency analysis: Is it worth the effort?,
15 Advances in Water Resources, 105, 144–153, doi:10.1016/j.advwatres.2017.05.002, 2017.
- 16 Schillereff, D. N., Chiverrell, R. C., Macdonald, N. and Hooke, J. M.: Flood stratigraphies in lake sediments: A review, Earth-
17 Science Reviews, 135, 17–37, doi:10.1016/j.earscirev.2014.03.011, 2014.
- 18 [Schubert,A., Lauterbach,S., Leipe,C., Scholz,V., Brauer,A., Tarasov,P.E.Anthropogenic and climate controls on vegetation](https://doi.org/10.1016/j.palaeo.2020.109976)
19 [changes between 1500 BCE and 500 CE reconstructed from a high-resolution pollen record from varved sediments of Lake](https://doi.org/10.1016/j.palaeo.2020.109976)
20 [Mondsee, Austria, Palaeogeography, Palaeoclimatology, Palaeoecology \(559\) https://doi.org/10.1016/j.palaeo.2020.109976](https://doi.org/10.1016/j.palaeo.2020.109976)
21 [2020](https://doi.org/10.1016/j.palaeo.2020.109976)
- 22
- 23 Serinaldi, F. and Kilsby, C. G.: Stationarity is undead: Uncertainty dominates the distribution of extremes, Advances in Water
24 Resources, 77, 17–36, doi:10.1016/j.advwatres.2014.12.013, 2015.
- 25 Stedinger, J. R. and Cohn, T. A.: Flood Frequency Analysis With Historical and Paleoflood Information, Water Resources
26 Research, 22(5), 785–793, doi:10.1029/WR022i005p00785, 1986.
- 27 Steffensen, I. G.: Reconstruction of large floods in Glomma through the Holocene - possible links to natural climate variability
28 and global atmospheric circulation (Rekonstruksjon av storflommer i Glomma gjennom holosen-mulige koblinger til naturlig
29 klimavariabilitet og global atmosfærisk sirkulasjon - in Norwegian), The University of Bergen, Bergen, 15 May., 2014.
- 30 Støren, E. N. and Paasche, Ø.: Scandinavian floods: From past observations to future trends, Global and Planetary Change,
31 113, 34–43, doi:10.1016/j.gloplacha.2013.12.002, 2014.
- 32 Støren, E. N., Dahl, S. O., Nesje, A. and Paasche, Ø.: Identifying the sedimentary imprint of high-frequency Holocene river
33 floods in lake sediments: development and application of a new method, Quaternary Science Reviews, 29(23–24), 3021–3033,
34 doi:10.1016/j.quascirev.2010.06.038, 2010.
- 35 Støren, E. N., Kolstad, E. W. and Paasche, Ø.: Linking past flood frequencies in Norway to regional atmospheric circulation
36 anomalies, Journal of Quaternary Science, 27(1), 71–80, doi:10.1002/jqs.1520, 2012.

- 1 Støren, E. W. N., Paasche, Ø., Hirt, A. M. and Kumari, M.: Magnetic and geochemical signatures of flood layers in a lake
2 system, *Geochemistry, Geophysics, Geosystems*, 17(10), 4236–4253, doi:10.1002/2016GC006540, 2016.
- 3 Swierczynski, T., Lauterbach, S., Dulski, P., Delgado, J., Merz, B. and Brauer, A.: Mid- to late Holocene flood frequency
4 changes in the northeastern Alps as recorded in varved sediments of Lake Mondsee (Upper Austria), *Quaternary Science
5 Reviews*, 80, 78–90, doi:10.1016/j.quascirev.2013.08.018, 2013.
- 6 Tarr, R. S.: A hint with respect to the origin of terraces in glaciated regions, *American Journal of Science*, s3-44(259), 59–61,
7 doi:10.2475/ajs.s3-44.259.59, 1892.
- 8 TEK17: Building regulations (Byggtkninsk forskrift TEK17 - in Norwegian). [online] Available from:
9 <https://dibk.no/byggereglene/byggtknisk-forskrift-tek17/7-2/>, 2018.
- 10 Velle, G., Bjune, A. E., Larsen, J. and Birks, H. J. B.: Holocene climate and environmental history of Brurskardstjørni, a lake
11 in the catchment of Øvre Heimdalsvatn, south-central Norway, *Hydrobiologia*, 642(1), 13–34, doi:10.1007/s10750-010-0153-
12 7, 2010.
- 13 Viglione, A.: nsRFA: Non-supervised Regional Frequency Analysis. R package version 0.7-11., [online] Available from:
14 <http://cran.r-project.org/package=nsRFA>, 2012.
- 15 Viglione, A., Merz, R., Salinas, J. L. and Blöschl, G.: Flood frequency hydrology: 3. A Bayesian analysis, *Water Resources
16 Research*, 49(2), 675–692, doi:10.1029/2011WR010782, 2013.
- 17 Vormoor, K., Lawrence, D., Schlichting, L., Wilson, D. and Wong, W. K.: Evidence for changes in the magnitude and
18 frequency of observed rainfall vs. snowmelt driven floods in Norway, *Journal of Hydrology*, 538, 33–48,
19 doi:10.1016/j.jhydrol.2016.03.066, 2016.
- 20 [Walker, M., Johnsen, S., Rasmussen, S. O., Popp, T., Steffensen, J.-P., Gibbard, P., Hoek, W., Lowe, J., Andrews, J., Björck,
21 S., Cwynar, L. C., Hughen, K., Kershaw, P., Kromer, B., Litt, T., Lowe, D. J., Nakagawa, T., Newnham, R., and Schwander,
22 J. Formal definition and dating of the GSSP \(Global Stratotype Section and Point\) for the base of the Holocene using the
23 Greenland NGRIP ice core, and selected auxiliary records. *J. Quaternary Sci.*, Vol. 24 pp. 3–17. ISSN 0267-8179, 2009](#)
- 24 Wellington, S. L. and Vinegar, H. J.: X-RAY COMPUTERIZED TOMOGRAPHY., *JPT, Journal of Petroleum Technology*,
25 39(8), 885–898, doi:10.2118/16983-PA, 1987.
- 26 Wilhelm, B., Ballesteros Canovas, J. A., Corella Aznar, J. P., Kämpf, L., Swierczynski, T., Stoffel, M., Støren, E. and Toonen,
27 W.: Recent advances in paleoflood hydrology: From new archives to data compilation and analysis, *Water Security*, 3(May),
28 1–8, doi:10.1016/j.wasec.2018.07.001, 2018.
- 29 Wirth, S. B., Glur, L., Gilli, A. and Anselmetti, F. S.: Holocene flood frequency across the Central Alps - solar forcing and
30 evidence for variations in North Atlantic atmospheric circulation, *Quaternary Science Reviews*, 80, 112–128,
31 doi:10.1016/j.quascirev.2013.09.002, 2013.
- 32 [Østmoe, A. -The Large flood of 1789: the weather system that led to the largest flood disaster in Norway \(Stor-ofsen 1789 :
33 værssystemet som førte til den største flomkatastrofen i Norge - in Norwegian\), *Oversiktsregisteret, Ski, Norway, 1985*](#)
- 34